67. Top Quark

Updated September 2017 by T.M. Liss (The City College of New York), F. Maltoni (Univ. Catholique de Louvain), and A. Quadt (Univ. Göttingen).

67.1. Introduction

In the Standard Model (SM), the left-handed top quark is the $Q = 2/3$, $T_3 = +1/2$ member of the weak-isospin doublet containing the bottom quark, while the right-handed top is an $SU(2)_L$ singlet (see the review on the "Electroweak Model and Constraints on New Physics" for more information). Its phenomenology is driven by its large mass. Being heavier than a W boson, it is the only quark that decays semi-weakly, i.e., into a real W boson and a b quark. Therefore, it has a very short lifetime and decays before hadronization can occur. In addition, it is the only quark whose Yukawa coupling to the Higgs boson is order of unity. For these reasons, the top quark plays a special role in the Standard Model and in many extensions thereof. Its phenomenology provides a unique laboratory where our understanding of the strong interactions, both in the perturbative and non-perturbative regimes, can be tested. An accurate knowledge of its properties (mass, couplings, production cross section, decay branching ratios, *etc.*) can bring key information on fundamental interactions at the electroweak symmetry-breaking scale and beyond. This review provides a concise discussion of the experimental and theoretical issues involved in the determination the top-quark properties.

67.2. Top-quark production at the Tevatron and LHC

In hadron collisions, top quarks are produced dominantly in pairs through the processes $q\overline{q} \to t\overline{t}$ and $gg \to t\overline{t}$, at leading order in QCD. Approximately 85% of the production cross section at the Tevatron ($p\bar{p}$ at 1.96 TeV) is from $q\overline{q}$ annihilation, with the remainder from gluon-gluon fusion, while at LHC (pp) energies about 90% of the production is from the latter process at $\sqrt{s} = 14$ TeV ($\approx 80\%$ at $\sqrt{s} = 7$ TeV).

Predictions for the top-quark production total cross sections are now available at next-to-next-to leading order (NNLO) with next-to-next-to-leading-log (NNLL) soft gluon resummation [1]. Assuming a top-quark mass of 173.3 GeV/c^2, close to the Tevatron + LHC average [2], the resulting theoretical prediction of the top-quark pair cross-section at NNLO+NNLL accuracy at the Tevatron at $\sqrt{s} = 1.96$ TeV is $\sigma_{t\bar{t}} = 7.16^{+0.11+0.17}_{-0.20-0.12}$ pb where the first uncertainty is from scale dependence and the second from parton distribution functions. At the LHC, assuming a top-quark mass of 172.5 GeV/c^2 the cross sections are: $\sigma_{t\bar{t}} = 177.3^{+4.6+9.0}_{-6.0-9.0}$ pb at $\sqrt{s} = 7$ TeV, $\sigma_{t\bar{t}} = 252.9^{+6.4+11.5}_{-8.6-11.5}$ pb at $\sqrt{s} = 8$ TeV, $\sigma_{t\bar{t}} = 831.8^{+19.8+35.1}_{-29.2-35.1}$ pb at $\sqrt{s} = 13$ TeV, and $\sigma_{t\bar{t}} = 984.5^{+23.2+41.3}_{-34.7-41.3}$ pb at $\sqrt{s} = 14$ TeV [1].

Electroweak single top-quark production mechanisms, namely from $q\overline{q}' \to t\overline{b}$ [3], $qb \to q't$ [4], mediated by virtual s-channel and t-channel W-bosons, and Wt-associated production, through $bg \to W^-t$, lead to somewhat smaller cross sections. For example, t-channel production, while suppressed by the weak coupling with respect to the strong pair production, is kinematically enhanced, resulting in a sizable cross section both at Tevatron and LHC energies. At the Tevatron, the t- and s-channel cross sections of top

and antitop are identical, while at the LHC they are not, due to the charge-asymmetric initial state. Approximate NNLO cross sections for t-channel single top-quark production ($t+\bar{t}$) are calculated for $m_t = 173.3$ GeV/c^2 to be $2.06^{+0.13}_{-0.13}$ pb in $p\overline{p}$ collisions at $\sqrt{s} = 1.96$ TeV (scale and parton distribution functions uncertainties are combined in quadrature) [5]. Recently, calculations at NNLO accuracy for the t-channel cross section at the LHC have appeared [6,7], predicting ($m_t = 172.5$ GeV/c^2): $\sigma_{t+\bar{t}} = 64.0^{+0.77}_{-0.38}$ pb at $\sqrt{s} = 7$ TeV, $\sigma_{t+\bar{t}} = 84.6^{+1.0}_{-0.51}$ pb at $\sqrt{s} = 8$ TeV, $\sigma_{t+\bar{t}} = 215^{+2.1}_{-1.3}$ pb at $\sqrt{s} = 13$ TeV, and $\sigma_{t+\bar{t}} = 245^{+2.7}_{-1.3}$ pb at $\sqrt{s} = 14$ TeV, where the quoted uncertainties are from scale variation only. For the s-channel, NNLO approximated calculations yield $1.03^{+0.05}_{-0.05}$ pb for the Tevatron, and $4.5^{+0.2}_{-0.2}(5.5^{+0.2}_{-0.2})$ pb for $\sqrt{s} = 7$ (8) TeV at the LHC, with 69% (31%) of top (anti-top) quarks [8]. While negligible at the Tevatron, at LHC energies the Wt-associated production becomes relevant. At $\sqrt{s} = 7$ (8) TeV, an approximate NNLO calculation gives $15.5^{+1.2}_{-1.2}(22.1^{+1.5}_{-1.5})$ pb ($t+\bar{t}$), with an equal proportion of top and anti-top quarks [9].

Assuming $|V_{tb}| \gg |V_{td}|, |V_{ts}|$ (see the review "The CKM Quark-Mixing Matrix" for more information), the cross sections for single top production are proportional to $|V_{tb}|^2$, and no extra hypothesis is needed on the number of quark families or on the unitarity of the CKM matrix in extracting $|V_{tb}|$. Separate measurements of the s- and t-channel processes provide sensitivity to physics beyond the Standard Model [10].

With a mass above the Wb threshold, and $|V_{tb}| \gg |V_{td}|$, $|V_{ts}|$, the decay width of the top quark is expected to be dominated by the two-body channel $t \to Wb$. Neglecting terms of order m_b^2/m_t^2, α_s^2, and $(\alpha_s/\pi)M_W^2/m_t^2$, the width predicted in the SM at NLO is [11]:

$$\Gamma_t = \frac{G_F m_t^3}{8\pi\sqrt{2}} \left(1 - \frac{M_W^2}{m_t^2}\right)^2 \left(1 + 2\frac{M_W^2}{m_t^2}\right) \left[1 - \frac{2\alpha_s}{3\pi}\left(\frac{2\pi^2}{3} - \frac{5}{2}\right)\right], \qquad (67.1)$$

where m_t refers to the top-quark pole mass. The width for a value of $m_t = 173.3$ GeV/c^2 is 1.35 GeV/c^2 (we use $\alpha_s(M_Z) = 0.118$) and increases with mass. With its correspondingly short lifetime of $\approx 0.5 \times 10^{-24}$ s, the top quark is expected to decay before top-flavored hadrons or $t\bar{t}$-quarkonium-bound states can form [12]. In fact, since the decay time is close to the would-be-resonance binding time, a peak will be visible in e^+e^- scattering at the $t\bar{t}$ threshold [13] and it is in principle present (yet very difficult to measure) in hadron collisions, too [14]. The order α_s^2 QCD corrections to Γ_t are also available [15], thereby improving the overall theoretical accuracy to better than 1%.

The final states for the leading pair-production process can be divided into three classes:

A. $t\bar{t} \to W^+ b\, W^- \bar{b} \to q\,\overline{q}'\, b\, q''\,\overline{q}'''\,\bar{b}$, (45.7%)
B. $t\bar{t} \to W^+ b\, W^- \bar{b} \to q\,\overline{q}'\, b\, \ell^-\,\overline{\nu}_\ell\,\bar{b} + \ell^+\,\nu_\ell\, b\, q''\,\overline{q}'''\,\bar{b}$, (43.8%)
C. $t\bar{t} \to W^+ b\, W^- \bar{b} \to \ell^+\,\nu_\ell\, b\, \ell'^-\,\overline{\nu}_{\ell'}\,\bar{b}$. (10.5%)

The quarks in the final state evolve into jets of hadrons. A, B, and C are referred to as the all-jets, lepton+jets (ℓ+jets), and dilepton ($\ell\ell$) channels, respectively. Their relative contributions, including hadronic corrections, are given in parentheses assuming lepton

universality. While ℓ in the above processes refers to e, μ, or τ, most of the analyses distinguish the e and μ from the τ channel, which is more difficult to reconstruct. Therefore, in what follows, we will use ℓ to refer to e or μ, unless otherwise noted. Here, typically leptonic decays of τ are included. In addition to the quarks resulting from the top-quark decays, extra QCD radiation (quarks and gluons) from the colored particles in the event can lead to extra jets.

The number of jets reconstructed in the detectors depends on the decay kinematics, as well as on the algorithm for reconstructing jets used by the analysis. Information on the transverse momenta of neutrinos is obtained from the imbalance in transverse momentum measured in each event (missing p_T, which is here also called missing E_T).

The identification of top quarks in the electroweak single top channel is much more difficult than in the QCD $t\bar{t}$ channel, due to a less distinctive signature and significantly larger backgrounds, mostly due to $t\bar{t}$ and W+jets production.

Fully exclusive predictions via Monte Carlo generators for the $t\bar{t}$ and single top production processes at NLO accuracy in QCD, including top-quark decays and possibly off-shell effects are available [16,17] through the MC@NLO [18] and POWHEG [19] methods.

Besides fully inclusive QCD or EW top-quark production, more exclusive final states can be accessed at hadron colliders, whose cross sections are typically much smaller, yet can provide key information on the properties of the top quark. For all relevant final states (*e.g.*, $t\bar{t}V$, $t\bar{t}VV$ with $V = \gamma, W, Z$, $t\bar{t}H, t\bar{t}$+jets, $t\bar{t}b\bar{b}, t\bar{t}t\bar{t}$) automatic or semi-automatic predictions at NLO accuracy in QCD also in the form of event generators, *i.e.*, interfaced to parton-shower programs, are available (see the review "Monte Carlo event generators" for more information).

67.3. Top-quark measurements

Since the discovery of the top quark, direct measurements of $t\bar{t}$ production have been made at five center-of-mass energies in pp or $p\bar{p}$ and one in pPb collisions, providing stringent tests of QCD. The first measurements were made in Run I at the Tevatron at $\sqrt{s} = 1.8$ TeV. In Run II at the Tevatron relatively precise measurements were made at $\sqrt{s} = 1.96$ TeV. Finally, beginning in 2010, measurements have been made at the LHC at $\sqrt{s} = 7$ TeV, $\sqrt{s} = 8$ TeV, and $\sqrt{s} = 13$ TeV, and recently also in a dedicated low energy run at $\sqrt{s} = 5.02$ TeV and at 8.16 TeV in pPb collisions.

Production of single top quarks through electroweak interactions has now been measured with good precision at the Tevatron at $\sqrt{s} = 1.96$ TeV, and at the LHC at $\sqrt{s} = 7$ TeV, $\sqrt{s} = 8$ TeV, and also at $\sqrt{s} = 13$ TeV. Measurements at the Tevatron have managed to separate the s- and t-channel production cross sections, and at the LHC, the Wt mechanism as well, though the t-channel is measured with best precision to date. The measurements allow an extraction of the CKM matrix element V_{tb}. Also more exclusive production modes and top-quark properties have been measured in single-top production.

With approximately 10 fb^{-1} of Tevatron data, and almost 5 fb^{-1} at 7 TeV, 20 fb^{-1} at 8 TeV and 36 fb^{-1} at 13 TeV at the LHC, many properties of the top quark have been measured with high precision. These include properties related to the production

mechanism, such as $t\bar{t}$ spin correlations, forward-backward or charge asymmetries, and differential production cross sections, as well as properties related to the tWb decay vertex, such as the helicity of the W-bosons from the top-quark decay. Recently, also studies of the $t\bar{t}\gamma$ and the $t\bar{t}Z$ interactions have been made. In addition, many searches for physics beyond the Standard Model or $t\bar{t}h$ or th production are being performed with increasing reach in both production and decay channels.

In the following sections we review the current status of measurements of the characteristics of the top quark.

67.3.1. *Top-quark production* :

67.3.1.1. $t\bar{t}$ *production:*

Fig. 67.1 summarizes the $t\bar{t}$ production cross-section measurements from both the Tevatron and LHC. Please note that some cross section measurements at the LHC have luminosity-related uncertainties which have improved in the meantime [20]. The most recent measurement from DØ [21]($p\bar{p}$ at $\sqrt{s} = 1.96$ TeV), combining the measurements from the dilepton and lepton plus jets final states in 9.7 fb^{-1}, is $7.26 \pm 0.13^{+0.57}_{-0.50}$ pb.

From CDF the most precise measurement made recently [22] is in 8.8 fb^{-1} in the dilepton channel requiring at least one b-tag, yielding 7.09 ± 0.84 pb. Both of these measurements assume a top-quark mass of 172.5 GeV/c^2. The dependence of the cross-section measurements on the value chosen for the mass is less than that of the theory calculations because it only affects the determination of the acceptance. In some analyses also the shape of topological variables might be modified.

Combining the recent cross section measurements with older ones in other channels yields $\sigma_{t\bar{t}} = 7.63 \pm 0.50$ pb (6.6%) for CDF, $\sigma_{t\bar{t}} = 7.56 \pm 0.59$ pb (7.8%) for DØ and $\sigma_{t\bar{t}} = 7.60 \pm 0.41$ pb (5.4%) for the Tevatron combination [23] in good agreement with the SM expectation of $7.35^{+0.28}_{-0.33}$ pb at NNLO+NNLL in perturbative QCD [1] for a top mass of 172.5 GeV. The contributions to the uncertainty are 0.20 pb from statistical sources, 0.29 pb from systematic sources, and 0.21 pb from the uncertainty on the integrated luminosity.

CDF has measured the $t\bar{t}$ production cross section in the dilepton channel with one hadronically decaying tau in 9.0 fb^{-1}, yielding $\sigma_{t\bar{t}} = 8.1 \pm 2.1$ pb. By separately identifying the single-tau and the ditau components, they measure the branching fraction of the top quark into the tau lepton, tau neutrino, and bottom quark to be (9.6 ± 2.8)% [24]. CDF also performs measurements of the $t\bar{t}$ production cross section normalized to the Z production cross section in order to reduce the impact of the luminosity uncertainty.

DØ has performed a measurement of differential $t\bar{t}$ cross sections in 9.7 fb^{-1} of lepton+jets data as a function of the transverse momentum and absolute value of the rapidity of the top quarks as well as of the invariant mass of the $t\bar{t}$ pair [25]. Observed differential cross sections are consistent with standard model predictions.

The LHC experiments ATLAS and CMS use similar techniques to measure the $t\bar{t}$ cross section in pp collisions. The most precise measurements come from the dilepton channel, and in particular the $e\mu$ channel. At $\sqrt{s} = 7$ TeV, ATLAS uses 4.6 fb^{-1}

of $e\mu$ events in which they select an extremely clean sample and determine the $t\bar{t}$ cross section simultaneously with the efficiency to reconstruct and tag b-jets, yielding $\sigma_{t\bar{t}} = 182.9 \pm 7.1$ pb, corresponding to 3.9% precision [26]. Other measurements by ATLAS at $\sqrt{s} = 7$ TeV, include a measurement in 0.7 fb^{-1} in the lepton+jets channel [27], in the dilepton channel [28], and in 1.02 fb^{-1} in the all-hadronic channel [29], which together yield a combined value of $\sigma_{t\bar{t}} = 177 \pm 3(stat.)^{+8}_{-7}(syst.) \pm 7(lumi.)$ pb (6.2%) assuming $m_t = 172.5$ GeV/c^2 [30]. In 4.7 fb^{-1} of all-jets events, they obtain $\sigma_{t\bar{t}} = 168 \pm 62$ pb [31]. Further analyses in the hadronic τ plus jets channel in 1.67 fb^{-1} [32] and the hadronic τ + lepton channel in 2.05 fb^{-1} [33], and the all-hadronic channel in 4.7 fb^{-1} [31] yield consistent albeit less precise results. The most precise measurement from CMS is also obtained in the dilepton channel, where they measure $\sigma_{t\bar{t}} = 162 \pm 2(stat.) \pm 5(syst.) \pm 4(lumi.)$ pb, corresponding to a 4.2% precision [34]. Other measurements at $\sqrt{s} = 7$ TeV from CMS include measurements with 2.3 fb^{-1} in the e/μ+jets channel [35], dilepton channel [34], with 3.5 fb^{-1} in the all-hadronic channel [36], with 2.2 fb^{-1} in the lepton+τ channel [37], and with 3.9 fb^{-1} in the τ+jets channel [38]. ATLAS and CMS also provide a combined cross section at $\sqrt{s} = 7$ TeV of $173.3 \pm 2.3(stat.) \pm 7.6(syst.) \pm 6.3(lumi.)$ pb using slightly older results based on $0.7 - 1.1$ fb^{-1} [39].

At $\sqrt{s} = 8$ TeV, ATLAS measures the $t\bar{t}$ cross section with 20.3 fb^{-1} using $e\mu$ dilepton events, with a simultaneous measurement of the $b-$tagging efficiency, yielding $\sigma_{t\bar{t}} = 242.4 \pm 1.7(stat.) \pm 5.5(syst.) \pm 7.5(lumi.) \pm 4.2(beam\,energy)$ pb [26] assuming $m_t = 172.5$ GeV/c^2, which corresponds to a 4.7% precision. In the lepton+jets channel, they measure $\sigma_{t\bar{t}} = 260 \pm 1(stat.)^{+20}_{-23}(syst.) \pm 8(lumi.) \pm 4(beam\,energy)$ pb [41] in 20.3 fb^{-1} using a likelihood discriminant fit and b-jet identification. Very recently, ATLAS performed a new analysis in 20.2 fb^{-1} lepton+jets events. They model the W+jets background using Z+jets data and employ neural networks in three jet-multiplicity and b-jet multiplicity regions for the signal and background separation, yielding $\sigma_{t\bar{t}} = 248.3 \pm 0.7(stat.) \pm 13.4(syst.) \pm 4.7(lumi.)$ pb [42]. Recently, ATLAS also performed a cross section measurement in the hadronic τ+jets channel yielding consistent, albeit less precise results [43]. CMS performs a template fit to the M_{lb} mass distribution using 19.6 fb^{-1} in the lepton+jets channel yielding $\sigma_{t\bar{t}} = 228.5 \pm 3.8(stat.) \pm 13.7(syst.) \pm 6(lumi.)$ pb [44]. These 8 TeV measurements are in agreement with QCD predictions up to next-to-next-to-leading order. In the $e\mu$ channel, using 19.7 fb^{-1}, the cross sections are extracted using a binned likelihood fit to multi-differential final state distributions related to identified b quark and other jets in the event, yielding $\sigma_{t\bar{t}} = 244.9 \pm 1.4(stat.)^{+6.3}_{-5.5}(sys.) \pm 6.4(lumi.)$ pb [46]. The cross section and its ratio between 7 TeV and 8 TeV measurements are found to be consistent with pQCD calculations. The cross section is also measured in the hadronic τ+jets channel, yielding $\sigma_{t\bar{t}} = 257 \pm 3(stat.) \pm 24(syst.) \pm 7(lumi.)$ pb [47] and in the all-jets final state giving $\sigma_{t\bar{t}} = 275.6 \pm 6.1(stat.) \pm 37.8(syst.) \pm 7.2(lumi.)$ pb [48]. In combination of the most precise $e\mu$ measurements in $5.3 - 20.3$ fb^{-1}, ATLAS and CMS together yield at 8 TeV $\sigma_{t\bar{t}} = 241.5 \pm 1.4(stat.) \pm 5.7(syst.) \pm 6.2(lumi.)$ pb [49], which corresponds to a 3.5% precision, challenging the precision of the corresponding theoretical predictions.

The LHCb collaboration presented the first observation of top-quark production in

the forward region in pp-collisions. The $W + b$ final state with $W \to \mu\nu$ is reconstructed using muons with a transverse momentum, p_T, larger than 25 GeV in the pseudorapidity range $2.0 < \eta < 4.5$. The b-jets are required to have 50 GeV $< \mathrm{p_T} <$ 100 GeV and $2.2 < \eta < 4.2$, while the transverse component of the sum of the muon and b-jet momenta must satisfy $p_T > 20$ GeV. The results are based on data corresponding to integrated luminosities of 1.0 and 2.0 fb^{-1} collected at center-of-mass energies of 7 and 8 TeV by LHCb. The inclusive top quark production cross sections in the fiducial region are $\sigma_{t\bar{t}} = 239 \pm 53(stat.) \pm 38(syst.)$ pb at 7 TeV, and $\sigma_{t\bar{t}} = 289 \pm 43(stat.) \pm 46(syst.)$ pb at 8 TeV [50].

ATLAS and CMS have also measured the $t\bar{t}$ production cross section with early Run-II data at $\sqrt{s} = 13$ TeV in $e\mu$ events with at least one b-tag. ATLAS uses 78 pb^{-1} and obtains $\sigma_{t\bar{t}} = 825 \pm 114$ pb [51]. CMS uses 42 pb^{-1} and measures $\sigma_{t\bar{t}} = 836 \pm 27(stat.) \pm 88(syst.) \pm 100(lumi.)$ pb [52]. Very recently, ATLAS used 3.2 fb^{-1} in the $e\mu$ channel, resulting in $\sigma_{t\bar{t}} = 818 \pm 8(stat.) \pm 27(syst.) \pm 19(lumi.) \pm 12(beam)$ pb, consistent with theoretical QCD calculations at NNLO [53].

A recent 'fiducial' measurement by ATLAS, corresponding to the experimental acceptance of the leptons uses 85 pb^{-1} of lepton+jets data and a simple counting approach. ATLAS measures a cross section of $\sigma_{t\bar{t}} = 817 \pm 13(stat.) \pm 103(syst.) \pm 88(lumi)$ pb [54]. CMS uses 2.2 fb^{-1} of $e\mu$ data with two or more jets and at least one b-tag, yielding $\sigma_{t\bar{t}} = 815 \pm 9(stat.) \pm 38(syst.) \pm 19(lumi.)$ pb, in agreement with the expectation from the standard model [55]. In 2.2 fb^{-1} of lepton+jets events, CMS performs a likelihood fit to the invariant mass distribution of the isolated lepton and the b-tagged jet in categories of jet multiplicity, resulting in $\sigma_{t\bar{t}} = 888 \pm 2(stat.)^{+26}_{-28}(syst.) \pm 20(lumi.)$ pb [56], in agreement with the standard model prediction. This result is also used to extract the top-quark mass. In the all-jets channel, CMS uses 2.53 fb^{-1} of data, yielding a cross section of $\sigma_{t\bar{t}} = 834 \pm 25(stat.) \pm 23(lumi.)$ pb [57]. Also differential cross sections as a function of the leading top quark transverse momentum are measured. The measured top quark p_T spectrum is found to be significantly softer than the theory predictions.

Recently, CMS has also measured the top-quark pair production cross section in a special LHC run with $\sqrt{s} = 5.02$ TeV, accumulating 27.4 pb^{-1}. The measurement is performed by analyzing events with at least one charged lepton. The measured cross section is $\sigma_{t\bar{t}} = 69.5 \pm 8.4$ pb [58], in agreement with the expectation from the standard model. In order to test consistency of the cross-section measurements with some systematic uncertainties cancelling out while testing pQCD and PDFs, cross-section ratios between mesurements at 7 TeV and at 8 TeV are performed and cited in several cases. In other cases, the cross-section ratio between $t\bar{t}$- and Z-production is determined as that is independent of luminosity uncertainties, but keeps its sensitivity to the ratio of gluon versus quark PDFs. These experimental results should be compared to the theoretical calculations at NNLO+NNLL that yield $7.16^{+0.20}_{-0.23}$ pb for top-quark mass of 173.3 GeV/c^2 [1] at $\sqrt{s} = 1.96$ TeV, and for top-quark mass of 173.2 GeV/c^2 $\sigma_{t\bar{t}} = 173.6^{+4.5+8.9}_{-5.9-8.9}$ pb at $\sqrt{s} = 7$ TeV, $\sigma_{t\bar{t}} = 247.7^{+6.3+11.5}_{-8.5-11.5}$ pb at $\sqrt{s} = 8$ TeV, and $\sigma_{t\bar{t}} = 816.0^{+19.4+34.4}_{-28.6-34.4}$ pb at $\sqrt{s} = 13$ TeV, at the LHC [1]. CMS also performed a measurement of top-quark pair production in pPb heavy ion collisions at $\sqrt{s} = 8.16$ TeV

in 174 nb^{-1} of lepton+jets events. They measure a cross section of $\sigma_{t\bar{t}} = 45 \pm 8$ pb, which is consistent with pQCD calculations and with the scaled pp data [59].

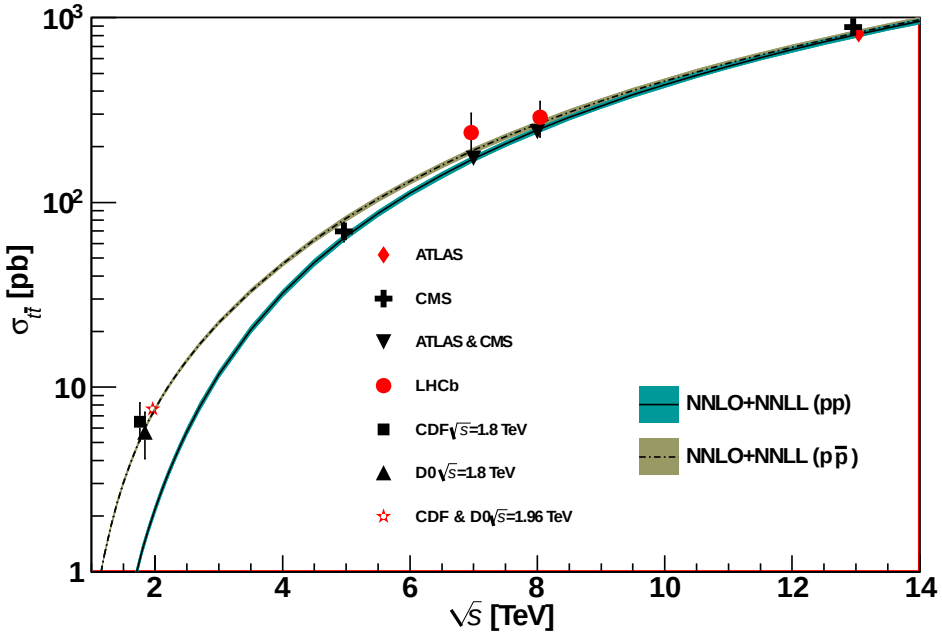

Figure 67.1: Measured and predicted $t\bar{t}$ production cross sections from Tevatron energies in $p\bar{p}$ collisions to LHC energies in pp collisions. Tevatron data points at $\sqrt{s} = 1.8$ TeV are from Refs. [63,64]. Those at $\sqrt{s} = 1.96$ TeV are from Refs. [21–23]. The ATLAS, CMS, and LHCb data points are from Refs. [26,34,39,40,45,49,50,53,56], and [58], respectively. Theory curves and uncertainties are generated using [1] for $m_t = 172.5$ GeV/c^2, the m_t value assumed in the cross-section measurements. Figure adapted from Ref. [60].

In Fig. 67.1, one sees the importance of $p\bar{p}$ at Tevatron energies where the valence antiquarks in the antiprotons contribute to the dominant $q\bar{q}$ production mechanism. At LHC energies, the dominant production mode is gluon-gluon fusion and the pp-$p\bar{p}$ difference nearly disappears. The excellent agreement of these measurements with the theory calculations is a strong validation of QCD and the soft-gluon resummation techniques employed in the calculations. The measurements reach high precision and provide stringent tests of pQCD calculations at NNLO+NNLL level including their respective PDF uncertainties.

Most of these measurements assume a $t \to Wb$ branching ratio of 100%. CDF and DØ have made direct measurements of the $t \to Wb$ branching ratio [61]. Comparing the number of events with 0, 1 and 2 tagged b jets in the lepton+jets channel, and also in the dilepton channel, using the known b-tagging efficiency, the ratio $R = B(t \to Wb)/\sum_{q=d,s,b} B(t \to Wq)$ can be extracted. In 5.4 fb^{-1} of data, DØ measures

$R = 0.90 \pm 0.04$, 2.5σ from unity. The currently most precise measurement was made by CMS in 19.7 fb^{-1} at $\sqrt{s} = 8$ TeV. They find $R = 1.014 \pm 0.003(stat.) \pm 0.032(syst.)$ and $R > 0.955$ at 95% C.L. [62]. A significant deviation of R from unity would imply either non-SM top-quark decay (for example a flavor-changing neutral-current decay), or a fourth generation of quarks.

Thanks to the large available event samples, the Tevatron and the LHC experiments also performed differential cross-section measurements in $t\bar{t}$ production. Such measurements are crucial, as they allow even more stringent tests of perturbative QCD as description of the production mechanism, allow the extraction or the use of PDF fits, and enhance the sensitivity to possible new physics contributions, especially now that NNLO predictions for the main differential observables in $t\bar{t}$ prediction have become available [65]. Furthermore, such measurements reduce the uncertainty in the description of $t\bar{t}$ production as background in Higgs physics and searches for rare processes or beyond Standard Model physics. Differential cross sections are typically measured by a selection of candidate events, their kinematic reconstruction and subsequent unfolding of the obtained event counts in bins of kinematic distributions in order to correct for detector resolution effects, acceptance and migration effects. In some cases a bin-by-bin unfolding is used, while other analyses use more sophisticated techniques.

Experiments at Tevatron and LHC measure the differential cross section with respect to the $t\bar{t}$ invariant mass, $d\sigma/dM_{t\bar{t}}$. The spectra are fully corrected for detector efficiency and resolution effects and are compared to several Monte Carlo simulations as well as selected theoretical calculations.

Using 9.45 fb^{-1}, CDF measured $d\sigma/dM_{t\bar{t}}$, in the lepton+jets channel providing sensitivity to a variety of exotic particles decaying into $t\bar{t}$ pairs [66]. In 9.7 fb^{-1} of lepton+jets data, DØ measured the differential $t\bar{t}$ production cross section with respect to the transverse momentum and absolute rapidity of the top quarks as well as of the invariant mass of the $t\bar{t}$ pair [25], which are all found to be in good agreement with the SM predictions.

ATLAS measured the differential $t\bar{t}$ production cross section with respect to the top-quark transverse momentum, and of the mass, transverse momentum and rapidity of the top quark, the antitop quark as well as the $t\bar{t}$ system in 4.6 fb^{-1} at $\sqrt{s} = 7$ TeV in the lepton+jets channel [67–69]. It is found that data is softer than all predictions for higher values of the mass of the $t\bar{t}$ system as well as in the tail of the top-quark p_T spectrum beginning at 200 GeV, particularly in the case of the `Alpgen`+`Herwig` generator. The $M_{t\bar{t}}$ spectrum is not well described by NLO+NNLL calculations and there are also disagreements between the measured rapidity of the $t\bar{t}$ system spectrum and the `MC@NLO`+`Herwig` and `POWHEG`+`Herwig` generators, both evaluated with the CT10 PDF set. All distributions show a preference for HERAPDF1.5 when used for the NLO QCD predictions. In 5.0 fb^{-1} of $\sqrt{s} = 7$ TeV data in the lepton+jets and the dilepton channels, CMS measured normalised differential $t\bar{t}$ cross sections with respect to kinematic properties of the final-state charged leptons and jets associated to b-quarks, as well as those of the top quarks and the $t\bar{t}$ system. The data are compared with several predictions from perturbative QCD calculations and found to be consistent [70].

ATLAS uses 4.6 fb^{-1} of data at 7 TeV and 20.2 fb^{-1} at 8 TeV to measure the

differential $t\bar{t}$ cross section as a function of the mass, the transverse momentum and the rapidity of the $t\bar{t}$ system [71]. The results are compared with different Monte Carlo generators and theoretical calculations of $t\bar{t}$ production and found to be consistent with the majority of predictions in a wide kinematic range. Using 20.3 fb^{-1} of $t\bar{t}$ events in the lepton+jets channel, ATLAS measures the normalized differential cross sections of $t\bar{t}$ production as a function of the top-quark, $t\bar{t}$ system and event-level kinematic observables [72]. The observables have been chosen to emphasize the $t\bar{t}$ production process and to be sensitive to effects of initial- and final-state radiation, to the different parton distribution functions, and to non-resonant processes and higher-order corrections. The results are in fair agreement with the predictions over a wide kinematic range. Nevertheless, most generators predict a harder top-quark transverse momentum distribution at high values than what is observed in the data. Predictions beyond NLO accuracy improve the agreement with data at high top-quark transverse momenta. Using the current settings in the Monte Carlo programs and parton distribution functions, the rapidity distributions are not well modelled by any generator under consideration. However, the level of agreement is improved when more recent sets of parton distribution functions are used. Recently, using 20.3 fb^{-1} of 8 TeV data, ATLAS performed a dedicated differential $t\bar{t}$ cross-section measurement of highly boosted top quarks in the lepton+jets channel, where the hadronically decaying top quark has a transverse momentum above 300 GeV [73]. Jet substructure techniques are employed to identify top quarks, which are reconstructed with an anti-k_t jet with a radius parameters $R = 1.0$. The predictions of NLO and LO matrix element plus parton shower Monte Carlo generators are found to generally overestimate the measured cross sections. Using 5.0 fb^{-1} of data at 7 TeV and 19.7 fb^{-1} at 8 TeV in the lepton+jets channel, CMS reports measurements of normalized differential cross sections for $t\bar{t}$ production with respect to four kinematic event variables: the missing transverse energy; the scalar sum of the jet transverse momentum (p_T); the scalar sum of the p_T of all objects in the event; and the p_T of leptonically decaying W bosons from top quark decays [74]. No significant deviations from the predictions of several standard model event generators are observed. Using the full 19.7 fb^{-1} data in the $e\mu$ channel, CMS measures normalized double-differential cross sections for $t\bar{t}$ production as a function of various pairs of observables characterizing the kinematics of the top quark and $t\bar{t}$ system [75]. The data are compared to calculations using perturbative quantum chromodynamics at NLO and approximate NNLO orders. They are also compared to predictions of Monte Carlo event generators that complement fixed-order computations with parton showers, hadronization, and multiple-parton interactions. Overall agreement is observed with the predictions, which is improved when the latest global sets (as determined here by CMS) of proton parton distribution functions are used. The inclusion of the measured $t\bar{t}$ cross sections in a fit of parametrized parton distribution functions is shown to have significant impact on the gluon distribution [75]. Another analysis at high transverse momentum regime for the top quarks, is performed by the CMS collaboration in 19.7 fb^{-1} at $\sqrt{s} = 8$ TeV [76]. The measurement is performed for events in electron/muon plus jets final states where the hadronically decaying top quark is reconstructed as a single large-radius jet and identified as a top candidate using jet substructure techniques. The integrated cross

section is measured at particle-level within a fiducial region resembling the detector-level selection as well as at parton-level. At particle-level, the fiducial cross section is measured to be $\sigma_{t\bar{t}} = 1.28 \pm 0.09(stat. + syst.) \pm 0.10(pdf) \pm 0.09(scales) \pm 0.03(lumi.)$ pb for $p_T >$ 400 GeV. At parton-level, it translates to $\sigma_{t\bar{t}} = 1.44 \pm 0.10(stat. + syst.) \pm 0.13(pdf) \pm 0.15(scales) \pm 0.04(lumi.)$ pb.

At parton-level, interations between incoming partons (quarks or gluons) are considered via a gauge interation yielding final state partons. While such interactions can be well described theoretically, partons are not visible in the detector. At the particle-level, visible and measurable hadrons, i.e. bound states of quarks and anti-quarks, are considered to form jets. The hadronisation process takes us from one level to the other.

Recently, in 19.7 fb^{-1} at $\sqrt{s} = 8$ TeV, CMS repeated those measurements in the lepton+jets and in the dilepton channels [77]. While the overall precision is improved, no significant deviations from the Standard Model are found, yet a softer spectrum for the top quark at high p_T with respect to theoretical available predictions has been observed. This behaviour has been also observed in the all-jets final state [78].

In 3.2 fb^{-1} at $\sqrt{s} = 13$ TeV, ATLAS measured the differential $t\bar{t}$ cross section as a function of the transverse momentum and absolute rapidity of the top quark, and of the transverse momentum, absolute rapidity and invariant mass of the $t\bar{t}$ system [79]. The measured differential cross sections are compared to predictions of NLO generators matched to parton showers and the measurements are found to be consistent with all models within the experimental uncertainties with the exception of the Powheg-Box+ Herwig++ predictions, which differ significantly from the data in both the transverse momentum of the top quark and the mass of the $t\bar{t}$ system. Using 3.2 fb^{-1} of data in the lepton+jets channel, ATLAS measured the differential cross sections of $t\bar{t}$ production in fiducial phase-spaces as a function of top-quark and $t\bar{t}$ system kinematic observables [81]. Two separate selections are applied that each focus on different top-quark momentum regions, referred to as resolved and boosted topologies of the $t\bar{t}$ final state. The measured spectra are corrected for detector effects and are compared to several Monte Carlo simulations by means of calculated χ^2 and p-values. At a center-of-mass energy of 13 TeV, ATLAS presents a measurement of the boosted top quark differential cross section in the all-hadronic decay mode [82]. They require two top-quark candidates, one with $p_T > 500$ GeV and a second with $p_T > 350$ GeV, with each candidate reconstructed as an anti-k_T jet with radius parameter $R = 1.0$. The top-quark candidates are separated from the multijet background using the jet substructure and the presence of a b-quark tag in each jet. The observed kinematic distributions are unfolded to recover the differential cross sections in a limited phase-space region and compared with Standard Model predictions, showing agreement.

In 2.1 fb^{-1} at $\sqrt{s} = 13$ TeV, CMS measures the normalized differential cross sections for $t\bar{t}$ production in the dilepton channels as a function of the kinematic properties of the leptons, jets from bottom quark hadronization, top quarks, and top quark pairs at the particle and parton levels [83]. The results are compared to several Monte Carlo generators that implement calculations up to next-to-leading order in perturbative quantum chromodynamics interfaced with parton showering, and also to fixed-order theoretical calculations of top quark pair production up to NNLO, showing agreement.

In 2.2 fb^{-1} of events in the lepton+jets channel, CMS measures the differential and double-differential cross sections for the $t\bar{t}$ production as a function of jet multiplicity and of kinematic variables of the top quarks and the $t\bar{t}$ system [84]. The differential cross sections are presented at particle level, within a phase space close to the experimental acceptance, and at parton level in the full phase space. The results are compared to several standard model predictions.

Further cross-section measurements are performed for $t\bar{t}$+ heavy flavour [85] and $t\bar{t}$+jets production as well as the differential measurement of the jet multiplicity in $t\bar{t}$ events [86,87]. Here, `MC@NLO`+`Herwig` MC is found to predict too few events at higher jet multiplicities. In addition, CMS measured the cross-section ratio $\sigma_{t\bar{t}b\bar{b}}/\sigma_{t\bar{t}jj}$ using 19.6 fb^{-1} of 8 TeV data [88]. This is of high relevance for top quark production as background to searches, for example for the ongoing search for $t\bar{t}h$ production. Very recently, ATLAS also measured the $t\bar{t}$ production cross section along with as the branching ratios into channels with leptons and quarks using 4.6 fb^{-1} of 7 TeV data [89]. They find agreement with the standard model at the level of a few percent.

67.3.1.2. *Single-top production:*

Single-top quark production was first observed in 2009 by DØ [90] and CDF [91,92] at the Tevatron. The production cross section at the Tevatron is roughly half that of the $t\bar{t}$ cross section, but the final state with a single W-boson and typically two jets is less distinct than that for $t\bar{t}$ and much more difficult to distinguish from the background of W+jets and other sources. A comprehensive review of the first observation and the techniques used to extract the signal from the backgrounds can be found in [93].

The dominant production at the Tevatron is through s-channel and t-channel W-boson exchange. Associated production with a W-boson (Wt production) has a cross section that is too small to observe at the Tevatron. The t-channel process is $qb \to q't$, while the s-channel process is $q\overline{q'} \to t\bar{b}$. The s- and t-channel productions can be separated kinematically. This is of particular interest because potential physics beyond the Standard Model, such as fourth-generation quarks, heavy W and Z bosons, flavor-changing-neutral-currents [10], or a charged Higgs boson, would affect the s- and t-channels differently. However, the separation is difficult and initial observations and measurements at the Tevatron by both experiments were of combined $s+t$-channel production. The two experiments combined their measurements for maximum precision with a resulting $s+t$-channel production cross section of $2.76^{+0.58}_{-0.47}$ pb [94]. The measured value assumes a top-quark mass of 170 GeV/c^2. The mass dependence of the result comes both from the acceptance dependence and from the $t\bar{t}$ background evaluation. Also the shape of discriminating topological variables is sensitive to m_t. The dependence on m_T is therefore not necessarily a simple linear dependence but amounts to only a few tenths of picobarns over the range $170 - 175$ GeV/c^2. The measured value agrees well with the theoretical calculation at $m_t = 173$ GeV/c^2 of $\sigma_{s+t} = 3.12$ pb (including both top and anti-top production) [5,8].

Using the full Run-II data set of up to 9.7 fb^{-1}, CDF and DØ have measured the t-channel single-top quark production to be $\sigma_{t+\bar{t}} = 2.25^{+0.29}_{-0.31}$ pb [96]. In the same publication, they also present the simultaneously measured $s-$ and $t-$channel cross

sections and the $s+t$ combined cross section measurement resulting in $\sigma_{s+t} = 3.30^{+0.52}_{-0.40}$ pb, without assuming the SM ratio of σ_s/σ_t. The modulus of the CKM matrix element obtained from the $s+t$-channel measurement is $|V_{tb}| = 1.02^{+0.06}_{-0.05}$ and its value is used to set a lower limit of $|V_{tb}| > 0.92$ at 95% C.L. Those results are in good agreement with the theoretical value at the mass 172.5 GeV/c^2 of $\sigma_t = 2.08 \pm 0.13$ pb [5]. It should be noted that the theory citations here list cross sections for t or $\overline{t}$ alone, whereas the experiments measure the sum. At the Tevatron, these cross sections are equal. The theory values quoted here already include this factor of two.

Using datasets of 9.7 fb^{-1} each, CDF and DØ combine their analyses and report the first observation of single-top-quark production in the s-channel, yielding $\sigma_s = 1.29^{+0.26}_{-0.24}$ pb [97]. The probability of observing a statistical fluctuation of the background of the given size is 1.8×10^{-10}, corresponding to a significance of 6.3 standard deviations.

At the LHC, the t-channel cross section is expected to be more than three times as large as s-channel and Wt production, combined. Both ATLAS and CMS have measured single top production cross sections at $\sqrt{s} = 7$ TeV in pp collisions (assuming $m_t = 172.5$ GeV/c^2 unless noted otherwise).

Using 4.59 fb^{-1} of data at $\sqrt{s} = 7$ TeV, ATLAS measures the t-channel single-top quark cross section in the lepton plus 2 or 3 jets channel with one b-tag by fitting the distribution of a multivariate discriminant constructed with a neural network, yielding $\sigma_t = 46 \pm 6$ pb, $\sigma_{\bar{t}} = 23 \pm 4$ pb with a ratio $R_t = \sigma_t/\sigma_{\bar{t}} = 2.04 \pm 0.18$ and $\sigma_{t+\bar{t}} = 68 \pm 8$ pb, consistent with SM expectations [98]. CMS follows two approaches in 1.6 fb^{-1} of lepton plus jets events. The first approach exploits the distributions of the pseudorapidity of the recoil jet and reconstructed top-quark mass using background estimates determined from control samples in data. The second approach is based on multivariate analysis techniques that probe the compatibility of the candidate events with the signal. They find $\sigma^{t-channel}_{t+\bar{t}} = 67.2 \pm 6.1$ pb, and $|V_{tb}| = 1.020 \pm 0.046(exp.) \pm 0.017(th.)$ [100].

At $\sqrt{s} = 8$ TeV, both experiments repeat and refine their measurements. ATLAS uses 20.2 fb^{-1} of data. Total, fiducial and differential cross-sections are measured for both top-quark and top-antiquark production [101]. An artificial neural network is employed to separate signal from background. The fiducial cross-section is measured with a precision of 5.8% (top quark) and 7.8% (top antiquark), respectively. The total cross-sections are measured to be $\sigma_t^{t-channel}(tq) = 56.7^{+4.3}_{-3.8}$ pb for top-quark production and $\sigma_{\bar{t}}^{t-channel}(\bar{t}q) = 32.9^{+3.0}_{-2.7}$ pb for top-antiquark production, in agreement with the Standard Model prediction. In addition, the ratio of top-quark to top-antiquark production cross-sections is determined to be $R_t = 1.72 \pm 0.09$. The total cross-section is used to extract the Wtb coupling: $f_{LV} \cdot |V_{tb}| = 1.029 \pm 0.048$, which corresponds to $|V_{tb}| > 0.92$ at the 95% confidence level, when assuming $f_{LV} = 1$ and restricting the range of $|V_{tb}|$ to the interval $[0, 1]$. The differential cross-sections as a function of the transverse momentum and rapidity of both the top quark and the top antiquark are measured at both the parton and particle levels. The transverse momentum and rapidity differential cross-sections of the accompanying jet from the t-channel scattering are measured at particle level. All measurements are compared

to various Monte Carlo predictions as well as to fixed-order QCD calculations where available. The SM predictions provide good descriptions of the data. CMS uses 19.7 fb^{-1} in the electron or muon plus jets channel, exploiting the pseudorapidity distribution of the recoil jet. They find $\sigma_t = 53.8 \pm 1.5(stat.) \pm 4.4(syst.)$ pb and $\sigma_{\bar{t}} = 27.6 \pm 1.3(stat.) \pm 3.7(syst.)$ pb, resulting in an inclusive t-channel cross section of $\sigma_{t+\bar{t}} = 83.6 \pm 2.3(stat.) \pm 7.4(syst.)$ [102]. They measure a cross section ratio of $R_t = \sigma_t/\sigma_{\bar{t}} = 1.95 \pm 0.10(stat.) \pm 0.19(syst.)$, in agreement with the SM. The CKM matrix element V_{tb} is extracted to be $|V_{tb}| = 0.998 \pm 0.038(exp.) \pm 0.016(th.)$. More recently, CMS has also provided a fiducial cross section measurement for t-channel single top at $\sqrt{s} = 8$ TeV with 19.7 fb^{-1} of data in signal events with exactly one muon or electron and two jets, one of which is associated with a b-hadron [103]. The definition of the fiducial phase space follows closely the constraints imposed by event-selection criteria and detector acceptance. The total fiducial cross section is measured using different generators at next-to-leading order plus parton-shower accuracy. Using as reference the `aMC@NLO` MC predictions in the four-flavour scheme a $\sigma_t^{\rm fid} = 3.38 \pm 0.25(exp.) \pm 0.20(th.)$ pb is obtained, in good agreement with the theory predictions. At 13 TeV, ATLAS uses 3.2 fb^{-1} to measurement the t-channel cross section. Using a binned maximum-likelihood fit to the discriminant distribution of a neural network, the cross-sections are determined to be $\sigma_t(tq) = 156 \pm 5(stat.) \pm 27(syst.) \pm 3(lumi.)$ pb and $\sigma(\bar{t}q) = 91 \pm 4(stat.) \pm 18(syst.) \pm 2(lumi.)$ pb [104]. The cross-section ratio is measured to be $R_t = \sigma_t/\sigma_{\bar{t}} = 1.72 \pm 0.09(stat.) \pm 0.18(syst.)$. All results are in agreement with Standard Model predictions.

A measurement of the t-channel single top-quark cross section is also available at 13 TeV with the CMS detector, corresponding to an integrated luminosity of 2.2 fb^{-1}. Fits to the transverse W-mass and the output of an artificial neural network allow the determination of the background and the signal contribution. The measured cross-section is $\sigma_t = 238 \pm 13 \pm 29$ pb [105]. The CKM matrix is determined to $|V_{tb}| = 1.05 \pm 0.07(exp.) \pm 0.02(th.)$.

The Wt process has a theoretical cross section of 15.6 ± 1.2 pb [9]. This is of interest because it probes the Wtb vertex in a different kinematic region than s- and t-channel production, and because of its similarity to the associated production of a charged-Higgs boson and a top quark. The signal is difficult to extract because of its similarity to the $t\bar{t}$ signature. Furthermore, it is difficult to uniquely define because at NLO a subset of diagrams have the same final state as $t\bar{t}$ and the two interfere [106]. The cross section is calculated using the *diagram removal* technique [107] to define the signal process. In the diagram removal technique the interfering diagrams are removed, at the amplitude level, from the signal definition (an alternative technique, *diagram subtraction* removes these diagrams at the cross-section level and yields similar results [107]) . These techniques work provided the selection cuts are defined such that the interference effects are small, which is usually the case.

Both, ATLAS and CMS, also provide evidence for the associate Wt production at $\sqrt{s} = 7$ TeV [108,109]. ATLAS uses 2.05 fb^{-1} in the dilepton plus missing E_T plus jets channel, where a template fit to the final classifier distributions resulting from boosted decision trees as signal to background separation is performed. The result is

incompatible with the background-only hypothesis at the 3.3σ (3.4σ expected) level, yielding $\sigma_{Wt} = 16.8 \pm 2.9(stat.) \pm 4.9(syst.)$ pb and $|V_{tb}| = 1.03^{+0.16}_{-0.19}$ [108]. CMS uses 4.9 fb^{-1} in the dilepton plus jets channel with at least one b-tag. A multivariate analysis based on kinematic properties is utilized to separate the $t\bar{t}$ background from the signal. The observed signal has a significance of 4.0σ and corresponds to a cross section of $\sigma_{Wt} = 16^{+5}_{-4}$ pb [109].

Both experiments repeated their Wt-analyses at $\sqrt{s} = 8$ TeV. ATLAS uses 20.3 fb^{-1} to select events with two leptons and one central b-jet. The Wt signal is separated from the backgrounds using boosted decision trees, each of which combines a number of discriminating variables into one classifier. Production of Wt events is observed with a significance of 7.7σ. The cross section is extracted in a profile likelihood fit to the classifier output distributions. The Wt cross section, inclusive of decay modes, is measured to be $\sigma_{Wt} = 23.0 \pm 1.3(stat.)^{+3.2}_{-3.5}(syst.) \pm 1.1(lumi.)$ pb, yielding a value for the CKM matrix element $|V_{tb}| = 1.01 \pm 0.10$ and a lower limit of 0.80 at the 95% C.L. [110]. A fiducial cross section is also measured. CMS uses 12.2 fb^{-1} in events with two leptons and a jet originated from a b quark. A multivariate analysis based on kinematic properties is utilized to separate the signal and background. The Wt associate production signal is observed at the level of 6.1σ, yielding $\sigma_{Wt} = 23.4 \pm 5.4$ pb and $|V_{tb}| = 1.03 \pm 0.12(exp.) \pm 0.04(th.)$ [111]. ATLAS and CMS also combine their measurements and obtain $\sigma_{Wt} = 25.0 \pm 1.4(stat.) \pm 4.4(syst.) \pm 0.7(lumi.)$ pb $= 25.0 \pm 4.7$ pb [112], in agreement with the NLO+NNLL expectation. They extract a 95% C.L. lower limit on the CKM matrix element of $|V_{tb}| > 0.79$.

At 13 TeV in the Wt-channel, ATLAS uses 3.2 fb^{-1} of events with two opposite sign isolated leptons and at least one jet; they are separated into signal and control regions based on their jet multiplicity and the number of jets with b-tags. Signal is separated from background in two regions using boosted decision trees. The cross section is extracted by fitting templates to the data distributions, and is measured to be $\sigma_{Wt} = 94 \pm 10(stat.)^{+28}_{-22}(syst.) \pm 2(lumi.)$ pb [113]. The measurement is in agreement with the Standard Model prediction. CMS uses 36 fb^{-1} of events with two opposite sign isolated leptons, one tight and one loose jet and one b-tag. Signal and background is separated in categories depending on the number of jets and the subset of b-tagged jets using a boosted decision tree. A maximum likelihood fits yields $\sigma_{Wt} = 63.1 \pm 6.6$ pb [114].

At ATLAS, a search for s-channel single top quark production is performed in 0.7 fb^{-1} at 7 TeV using events containing one lepton, missing transverse energy and two b-jets. Using a cut-based analysis, an observed (expected) upper limit at 95% C.L. on the s-channel cross-section of $\sigma_s < 26.5$ (20.5) pb is obtained [115]. In 8 TeV data, both ATLAS and CMS search for s-channel production. ATLAS uses 20.3 fb^{-1} of data with one lepton, large missing transverse momentum and exactly two b-tagged jets. They perform a maximum-likelihood fit of a discriminant based on a Matrix Element Method and optimized in order to separate single top-quark s-channel events from the main background contributions which are top-quark pair production and W boson production in association with heavy flavour jets. They find $\sigma_s = 4.8 \pm 0.8(stat.)^{+1.6}_{-1.3}(syst.)$ pb with a signal significance of 3.2 standard deviations [116], which provides first evidence for

s-channel single-top production at 8 TeV. The signal is extracted through a maximum-likelihood fit to the distribution of a multivariate discriminant defined using boosted decision trees to separate the expected signal contribution from background processes. At 7 TeV and 8 TeV, CMS uses 5.1 fb^{-1} and 19.3 fb^{-1}, respectively, and analyses leptonic decay modes by performing a maximum likelihood fit to a multivariate discriminant defined using a Boosted Decision Tree, yielding cross sections of $\sigma_s = 7.1 \pm 8.1$ pb and $\sigma_s = 13.4 \pm 7.3$ pb, respectively, and a best fit value of 2.0 ± 0.9 for the combined ratio of the measured σ_s values and the ones expected in the Standard Model [117]. The signal significance is 2.5 standard deviations. Both, ATLAS and CMS, also measured the electroweak production of singel top-quarks in association with a Z-boson, see section C.2.4 of this review.

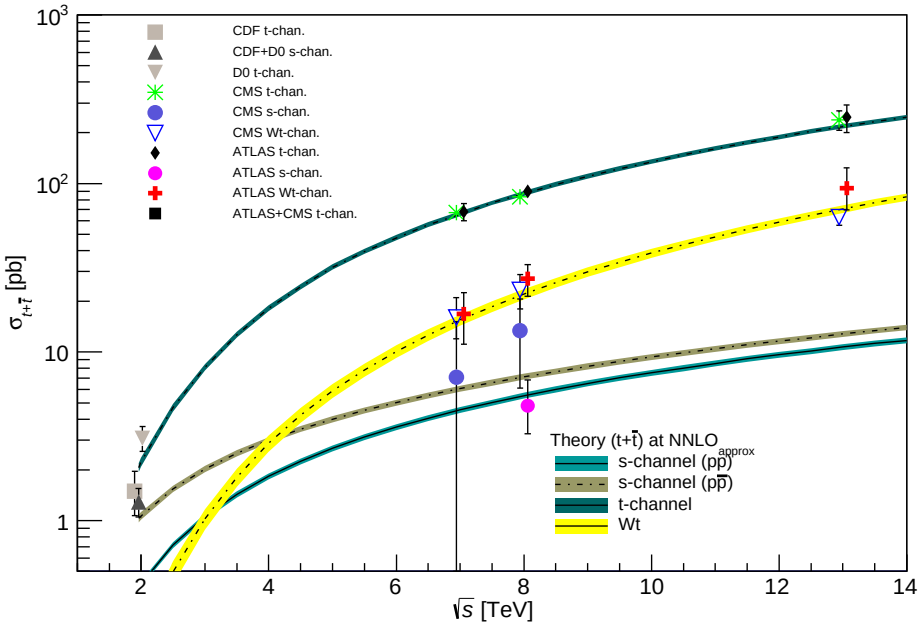

Figure 67.2: Measured and predicted single top production cross sections from Tevatron energies in $p\overline{p}$ collisions to LHC energies in pp collisions. Tevatron data points at $\sqrt{s} = 1.96$ TeV are from Refs. [96,97]. The ATLAS and CMS data points at $\sqrt{s} = 7$ TeV are from Refs. [98,100,108,109,115,117]. The ones at $\sqrt{s} = 8$ TeV are from Refs. [101,102,110,111,116,117]. The ones at $\sqrt{s} = 13$ TeV are from Refs. [104,105] Theory curves are generated using [5,8,9].

Fig. 67.2 provides a summary of all single top cross-section measurements at the Tevatron and the LHC as a function of the center-of-mass energy. All cross-section measurements are very well described by the theory calculation within their uncertainty.

Thanks to the large statistics now available at the LHC, both CMS and ATLAS experiments also performed differential cross-section measurements in single-top t-channel

production [98], [118]. Such measurements are extremely useful as they test our understanding of both QCD and EW top-quark interactions. The CMS collaboration has measured differential single top quark t-channel production cross sections as functions of the transverse momentum and the absolute value of the rapidity of the top quark. The analysis is performed in the leptonic decay channels of the top quark, with either a muon or an electron in the final state, using data collected with the CMS experiment at the LHC at $\sqrt{s} = 8$ TeV and corresponding to an integrated luminosity of 19.7 fb^{-1}. Neural networks are used to discriminate the signal process from the various background contributions. The results are found to agree with predictions from Monte Carlo generators [118]. Using the same data set and under the assumption that the spin analyzing power of a charged lepton is 100% as predicted in the SM, they are also able to measure the polarization of the top quark $P_t = 0.82 \pm 0.12(stat.) \pm 0.32(syst.)$ [119]. At 13 TeV, CMS measures the differential t-channel cross section with respect to the transverse momentum or the rapidity of the top- or the antitop-quark [120]. ATLAS has measured the differential Wt cross section in 36.1 fb^{-1} at 13 TeV with respect to the energy of the b-jet, the energy of the system of the two leptons and b-jet, and the transverse mass or mass of combinations of leptons, the b-jet and neutrinos [121].

67.3.1.3. *Top-Quark Forward-Backward & Charge Asymmetry:*

A forward-backward asymmetry in $t\bar{t}$ production at a $p\overline{p}$ collider arises starting at order α_S^3 in QCD from the interference between the Born amplitude $q\overline{q} \to t\bar{t}$ with 1-loop box production diagrams and between diagrams with initial- and final-state gluon radiation. The asymmetry, A_{FB}, is defined by

$$A_{FB} = \frac{N(\Delta y > 0) - N(\Delta y < 0)}{N(\Delta y > 0) + N(\Delta y < 0)}, \tag{67.2}$$

where $\Delta y = y_t - y_{\overline{t}}$ is the rapidity difference between the top- and the anti-top quark. Calculations at α_S^3 predict a small A_{FB} at the Tevatron. The most recent calculations up to order α_S^4, including electromagnetic and electroweak corrections, yield a predicted asymmetry of ($\approx$(9.5 $\pm$ 0.7)% [122]. This is about 10% higher than the previous calculation at NLO [123,124], and improves the agreement with experiment.

Both CDF and DØ measured asymmetry values in excess of the SM prediction, fueling speculation about exotic production mechanisms (see, for example, [125] and references therein). The first measurement of this asymmetry by DØ in 0.9 fb^{-1} [126] found an asymmetry at the detector level of (12 $\pm$ 8)%. The first CDF measurement in 1.9 fb^{-1} [127] yielded (24 $\pm$ 14)% at parton level. Both values were higher, though statistically consistent with the SM expectation. With the addition of more data, the uncertainties have been reduced, and the central values, if somewhat smaller, have remained consistent with the first measurements. At the same time, the improved calculations from theory have increased the predicted asymmetry values to the point where the discrepancy is no longer statistically significant.

CDF and DØ have now combined results using the full Tevatron dataset at $\sqrt{s} = 1.96$ TeV [128]. Three combined asymmetries are reported: $A_{FB}^{t\bar{t}}$ as defined in Eq. 2 for

fully-reconstructed $t\bar{t}$ events, a single-lepton asymmetry, A^{ℓ}_{FB} defined as in Eq. 2 but with Δy replaced by the product of the lepton charge and pseudo-rapidity, and a dilepton asymmetry, $A^{\ell\ell}_{FB}$, defined as in Eq. 2 but with Δy replaced by $\Delta\eta$ between the two leptons. The combined results are $A^{t\bar{t}}_{FB} = 0.128 \pm 0.021 \pm 0.014$, $A^{\ell}_{FB} = 0.073 \pm 0.016 \pm 0.012$, and $A^{\ell\ell}_{FB} = 0.108 \pm 0.043 \pm 0.016$. In each case the first uncertainty is statistical and the second systematic. These are to be compared to SM predictions at NNLO QCD and NLO electroweak of $A^{t\bar{t}}_{FB} = 0.095 \pm 0.007$ [122], $A^{\ell}_{FB} = 0.038 \pm 0.003$, and $A^{\ell\ell}_{FB} = 0.048 \pm 0.004$ [124], respectively. Both experiments have also measured differential asymmetries, in bins of $M_{t\bar{t}}$, Δy, $q_\ell \times \eta_\ell$, and $\Delta\eta_{\ell\ell}$, with consistent results, though the growth of $A^{t\bar{t}}_{FB}$ with increasing $M_{t\bar{t}}$ and Δy appears somewhat more rapid than the SM prediction [128].

At the LHC, where the dominant $t\bar{t}$ production mechanism is the charge-symmetric gluon-gluon fusion, the measurement is more difficult. For the sub-dominant $q\bar{q}$ production mechanism, the symmetric pp collision does not define a forward and backward direction. Instead, the charge asymmetry, A_C, is defined in terms of a positive versus a negative $t - \bar{t}$ rapidity difference, Δy

$$A^{t\bar{t}}_C = \frac{N(\Delta|y| > 0) - N(\Delta|y| < 0)}{N(\Delta|y| > 0) + N(\Delta|y| < 0)}. \tag{67.3}$$

Both CMS and ATLAS have measured A_C in the LHC dataset. Using lepton+jets events in 4.7 fb^{-1} of data at $\sqrt{s} = 7$ TeV, ATLAS measures $A^{t\bar{t}}_C = (0.6 \pm 1.0)\%$ [129]. ATLAS has reported on the same measurement performed at $\sqrt{s} = 8$ TeV with at 20.3 fb^{-1} of data, with a result of $A^{t\bar{t}}_C = (0.009 \pm 0.005)$ [130]. In the dilepton channel at $\sqrt{s} = 8$ TeV, ATLAS measures [131] $A^{t\bar{t}}_C = 0.021 \pm 0.016$, and $A^{\ell\ell}_C = 0.008 \pm 0.006$ (defined in terms of the $\Delta\eta$ of the two leptons) in agreement with the SM predictions of $(1.11 \pm 0.04)\%$ and $(0.64 \pm 0.03)\%$, respectively [124]. CMS, in 5.0 (19.7) fb^{-1} of $\sqrt{s} = 7(8)$ TeV data uses lepton+jets events to measure $A^{t\bar{t}}_C = (0.4 \pm 1.5)\%$ ($A^{t\bar{t}}_C = (0.33 \pm 0.26(stat.) \pm 0.33(syst.))\%$) [132,133]. Both measurements are consistent with the SM expectations of $A^{t\bar{t}}_C = 1.23 \pm 0.05\%$ at $\sqrt{s} = 7$ TeV and $1.11 \pm 0.04\%$ at $\sqrt{s} = 8$ TeV [124], although the uncertainties are still too large for a precision test. In 19.5 fb^{-1} of dilepton events at $\sqrt{s} = 8$ TeV, CMS measures $A^{t\bar{t}}_C = 0.011 \pm .013$ and $A^{\ell\ell}_C = 0.003 \pm 0.007$, consistent with SM expectations [124].

In their 7 and 8 TeV analyses ATLAS and CMS also provide differential measurements as a function of $M_{t\bar{t}}$ and the transverse momentum p_T and rapidity y of the $t\bar{t}$ system. To reduce model-dependence, the CMS Collaboration has performed a measurement in a reduced fiducial phase space [134], with a result of $A_C = -0.0035 \pm 0.0072(stat.) \pm 0.0031(syst.)$, in agreement with SM expectations.

To specifically address the dependence of the asymmetry on $M_{t\bar{t}}$, ATLAS has performed a measurement in boosted $t\bar{t}$ events [135]. In 20.3 fb^{-1} of data at $\sqrt{s} = 8$ TeV, in events with $M_{t\bar{t}} > 0.75$ TeV, and $|(\Delta|y|)| < 2$, ATLAS measures $A^{t\bar{t}}_C = (4.2 \pm 3.2)\%$ compared to a NLO SM prediction of $(1.60 \pm 0.04)\%$. The measurement is also presented in three bins of $M_{t\bar{t}}$, each in agreement, though with large uncertainties, with the SM expectations.

Both ATLAS and CMS have measured asymmetries in the distribution of leptons from $t\bar{t}$ decays. ATLAS, in 4.6 fb^{-1} of $\sqrt{s} = 7$ TeV data, has measured $A^{\ell\ell} = (2.4 \pm 1.5 \pm 0.9)\%$ in dilepton events [136]. Using a neutrino weighting technique in the same dataset to reconstruct the top quarks, ATLAS measures $A_C = (2.1 \pm 2.5 \pm 1.7)\%$. CMS, in 5.0 fb^{-1} of $\sqrt{s} = 7$ TeV data, uses dilepton events to measure $A_C = (1.0 \pm 1.5 \pm 0.6)\%$, where a matrix weighting technique is used to reconstruct the top quarks, and $A^{\ell\ell} = (0.9 \pm 1.0 \pm 0.6)\%$ [137]. An earlier result using lepton+jets events from the same CMS dataset found $A_C = (0.4 \pm 1.0 \pm 1.1)\%$ [132]. Combined results from ATLAS and CMS have recently been released [138]. At $\sqrt{s} = 7$ TeV the combined result is $A_C = (0.5 \pm 0.7 \pm 0.6)\%$, and at $\sqrt{s} = 8$ TeV it is $A_C = (0.55 \pm 0.23 \pm 0.25)\%$. These results are all consistent, within their large uncertainties, with the SM expectations of $A^{\ell\ell} = (0.70 \pm 0.03)\%$ and $A_C = (1.23 \pm 0.05)\%$ [124].

A model-independent comparison of the Tevatron and LHC results is made difficult by the differing $t\bar{t}$ production mechanisms at work at the two accelerators and by the symmetric nature of the pp collisions at the LHC. Given a particular model of BSM physics, a comparison can be obtained through the resulting asymmetry predicted by the model at the two machines, see for example [135].

67.3.2. *Top-Quark Properties* :

67.3.2.1. *Top-Quark Mass Measurements:*

The most precisely studied property of the top quark is its mass. The top-quark mass has been measured in the lepton+jets, the dilepton, and the all-jets channel by all four Tevatron and LHC experiments. The latest and/or most precise results are summarized in Table 67.1. The lepton+jets channel yields the most precise single measurements because of good signal to background ratio (in particular after b-tagging) and the presence of only a single neutrino in the final state. The momentum of a single neutrino can be reconstructed (up to a quadratic ambiguity) via the missing E_T measurement and the constraint that the lepton and neutrino momenta reconstruct to the known W boson mass. In the large data samples available at the LHC, measurements in the dilepton channel can be competitive and certainly complementary to those in the lepton+jets final state.

A large number of techniques have now been applied to measuring the top-quark mass. The original 'template method' [143], in which Monte Carlo templates of reconstructed mass distributions are fit to data, has evolved into a precision tool in the lepton+jets channel, where the systematic uncertainty due to the jet energy scale (JES) uncertainty is controlled by a simultaneous, *in situ* fit to the $W \to jj$ hypothesis [144]. All the latest measurements in the lepton+jets and the all-jets channels use this technique in one way or another. In 4.6 fb^{-1} of data at $\sqrt{s} = 7$ TeV in the lepton+jets channel, ATLAS achieves a total uncertainty of 0.73% with a statistical component of 0.44% [145]. The measurement is based on a 3-dimensional template fit, determining the top-quark mass, the global jet energy scale and a b-to-light jet energy scale factor. The most precise CMS result in the lepton+jets channel uses an ideogram method and comes from a so-called 'hybrid' approach in which the prior knowledge about the jet energy scale is incorporated as a Gaussian constraint, with a width determined by the uncertainty on the jet energy

Table 67.1: Measurements of top-quark mass from Tevatron and LHC. $\int \mathcal{L}dt$ is given in fb^{-1}. The results are a selection of both published and preliminary (not yet submitted for publication as of August 2017) measurements. For a complete set of published results see the Listings. Statistical uncertainties are listed first, followed by systematic uncertainties.

m_t (GeV/c^2)	Source	$\int \mathcal{L}dt$	Ref.	Channel
$172.99 \pm 0.48 \pm 0.78$	ATLAS	4.6	[145]	ℓ+jets+$\ell\ell$
$172.44 \pm 0.13 \pm 0.47$	CMS	19.7	[146]	ℓ+jets+$\ell\ell$+All jets
$172.35 \pm 0.16 \pm 0.48$	CMS	19.7	[146]	ℓ+jets
$172.22 \pm 0.18^{+0.89}_{-0.93}$	CMS	19.7	[152]	$\ell\ell$
$173.72 \pm 0.55 \pm 1.01$	ATLAS	20.2	[158]	All jets
$172.25 \pm 0.08 \pm 0.62$	CMS	35.9	[159]	ℓ+jets
$174.30 \pm 0.35 \pm 0.54$	CDF,DØ (I+II)	$\leq$9.7	[174]	publ. or prelim.
$173.34 \pm 0.27 \pm 0.71$	Tevatron+LHC	$\leq$8.7+$\leq$4.9	[2]	publ. or prelim.

corrections. In 19.7 fb^{-1} of $\sqrt{s} = 8$ TeV data, CMS achieves a total uncertainty of 0.30% with a statistical component of 0.09% with the hybrid approach [146]. Using this same method, CMS has recently released the first top-mass measurement from $\sqrt{s} = 13$ TeV data. Using 35.9 fb^{-1} of lepton+jets events they measure the top mass with a precision of 0.36%, with a statistical component of 0.05%.

The template method is complemented by the 'matrix element' method. This method was first applied by the DØ Collaboration [147], and is similar to a technique originally suggested by Kondo *et al.* [148] and Dalitz and Goldstein [149]. In the matrix element method a probability for each event is calculated as a function of the top-quark mass, using a LO matrix element for the production and decay of $t\bar{t}$ pairs. The *in situ* calibration of dijet pairs to the $W \to jj$ hypothesis is now also used with the matrix element technique to constrain the jet energy scale uncertainty. In the lepton+jets channel, DØ uses the full Tevatron dataset of 9.7 fb^{-1} and yields an uncertainty of about 0.43% [150].

In the dilepton channel, the signal to background is typically very good, but reconstruction of the mass is non-trivial because there are two neutrinos in the final state, yielding a kinematically unconstrained system. A variety of techniques have been developed to handle this. An analytic solution to the problem has been proposed [151], but this has not yet been used in the mass measurement. One of the most precise measurements in the dilepton channel comes from using the invariant mass of the charged

lepton and b-quark system ($M_{\ell b}$), which is sensitive to the top-quark mass and avoids the kinematic difficulties of the two-neutrino final state. In 4.6 fb^{-1} of $\sqrt{s} = 7$ TeV data, ATLAS has measured the top-quark mass in the dilepton channel to a precision of 0.81% using a template fit to the $M_{\ell b}$ distribution [145]. Recently, using 19.7 fb^{-1} of data at $\sqrt{s} = 8$ TeV, CMS has released [152] a mass measurement in the dilepton channel based on a simultaneous fit to $M_{\ell b}$ and a transverse-mass-like variable M_{T2} [153]. The most precise result in this analysis, which comes from a linear combination of fits with the jet energy scale fixed at its nominal value and one that simultaneously determines the top mass and jet energy scale, has a total uncertainty of 0.54%. At the LHC, because of their precision, these techniques have largely displaced a number of earlier techniques in the dilepton channel, though these techniques are still included, and described, in the combined results from CMS, reported in Ref. [146].

In the neutrino weighting technique, used by CDF to analyze the full Run 2 dilepton dataset of 9.1 fb^{-1}, a weight is assigned by assuming a top-quark mass value and applying energy-momentum conservation to the top-quark decay, resulting in up to four possible pairs of solutions for the neutrino and anti-neutrino momenta. The missing E_T calculated in this way is then compared to the observed missing E_T to assign a weight [156]. The CDF result achieves a precision of 1.8% using a combination of neutrino weighting and an "alternative mass", which is insensitive to the jet energy scale [157]. The alternative mass depends on the angles between the leptons and the leading jets and the lepton four-momenta.

In the all-jets channel there is no ambiguity due to neutrino momenta, but the signal to background is significantly poorer due to the severe QCD multijets background. The emphasis therefore has been on background modeling, and reduction through event selection. The most recent measurement in the all-jets channel, by CMS in 18.2 fb^{-1} of $\sqrt{s} = 8$ TeV data [146], uses an ideogram method and a 2-dimensional simultaneous fit for m_t and the jet energy scale to extract the top-quark mass and achieves a precision of 0.56%. A recent measurement from ATLAS [158] uses a template fit to the ratio of three-jet (m_t) to two-jet (M_W) mass in the all-hadronic channel, the two-jet denominator provides an *in situ*, fit to the $W \to jj$ hypothesis. In 20.2 fb^{-1} of data at $\sqrt{s} = 8$ TeV, the result has a precision of 0.65%. A measurement from CDF in 9.3 fb^{-1} uses a two-dimensional template fit and achieves a precision of 1.1% [160].

The CMS Collaboration has, for the first time, extracted a top-quark mass measurement from single-top events [161], something not previously done because of the poor signal to background ratio. The mass is extracted from the invariant mass of the muon, bottom quark, and missing transverse energy. In 19.7 fb^{-1} of data at $\sqrt{s} = 8$ TeV, a precision of 0.71% is achieved.

A dominant systematic uncertainty in these methods is the understanding of the jet energy scale, and so several techniques have been developed that have little sensitivity to the jet energy scale uncertainty. In addition to Reference [157] mentioned above, these include the measurement of the top-quark mass using the following techniques: Fitting of the lepton p_T spectrum of candidate events [162]; fitting of the transverse decay length of the b-jet (L_{xy}) [163]; fitting the invariant mass of a lepton from the W-decay and a muon from the semileptonic b decay [168], kinematic properties of secondary vertices

from $b-$quark fragmentation [164], the invariant mass of the $J/\psi + \ell$ system in events in which a $b-$quark fragments to a J/ψ particle [165], fitting the $b-$jet energy peak [166], and dilepton kinematics in $e\mu$ events citetopquark:CMS-PAS-TOP-16-002.

Several measurements have now been made in which the top-quark mass is extracted from the measured $t\bar{t}$ cross section using the theoretical relationship between the mass and the production cross section. These determinations make use of predictions calculated at higher orders, where the top mass enters as an input parameter defined in a given scheme. At variance with the usual methods, which involve the kinematic properties of the final states and therefore the pole mass, this approach can also directly determine a short-distance mass, such as the $\overline{\rm MS}$ mass [169]. With an alternative method ATLAS recently extracted the top-quark pole mass using $t\bar{t}$ events with at least one additional jet, basing the measurement on the relationship between the differential rate of gluon radiation and the mass of the quark [170]. A similar analysis by CMS used the differential cross section as a function of the invariant mass of the $t\bar{t}$ system and the leading jet not associated with the top decays [171].

Each of the experiments has produced a measurement combining its various results. The combined measurement from CMS with up to 19.7 fb^{-1} of data achieves statistical and systematic uncertainties of 0.08% and 0.27%, respectively [146]. The combined measurement from ATLAS, with 4.6 fb^{-1} yields statistical and systematic uncertainties of 0.28% and 0.45%, respectively [145]. CDF has combined measurements with up to 9.3 fb^{-1} [172] and achieves a statistical precision of 0.33% and a systematic uncertainty of 0.43%. DØ achieves a 0.33% statistical+JES and a 0.28% systematic uncertainty by combining results in 9.7 fb^{-1} [173].

Combined measurements from the Tevatron experiments and from the LHC experiments take into account the correlations between different measurements from a single experiment and between measurements from different experiments. The Tevatron average [174], using up to 9.7 fb^{-1} of data, now has a precision of 0.37%. The LHC combination, using up to 4.9 fb^{-1} of data, has a precision of 0.56% [175], where more work on systematic uncertainties is required. A Tevatron-LHC combination has been released, combining the results of all four experiments, using the full Tevatron dataset and the $\sqrt{s} = 7$ TeV LHC data, with a resulting precision of 0.44% [2]

The direct measurements of the top-quark mass, such as those shown in Table 67.1, correspond to the parameter used in the Monte Carlo generators, which is generally agreed to be the pole mass. The relation between the pole mass and short-distance masses, such as $\overline{\rm MS}$, is affected by non-perturbative effects. Recent calculations evaluate the size of this ambiguity to be below 250 MeV and therefore still smaller than the current measurement uncertainty [176,177].

With the discovery of a Higgs boson at the LHC with a mass of about 125 GeV/c^2 [178,179], the precision measurement of the top-quark mass takes a central role in the question of the stability of the electroweak vacuum because top-quark radiative corrections tend to drive the Higgs quartic coupling, λ, negative, potentially leading to an unstable vacuum. A recent calculation at NNLO [180] leads to the conclusion of vacuum stability for a Higgs mass satisfying $M_H \geq 129.4 \pm 5.6$ GeV/c^2 [181]. Given the uncertainty, a Higgs mass of 126 GeV/c^2 satisfies the limit, but the central values of

the Higgs and top-quark masses put the electroweak vacuum squarely in the metastable region. The uncertainty is dominated by the precision of the top-quark mass measurement and its interpretation as the pole mass. For more details, see the Higgs boson review in this volume.

As a test of the CPT-symmetry, the mass difference of top- and antitop-quarks $\Delta m_t = m_t - m_{\bar{t}}$, which is expected to be zero, can be measured. CDF measures the mass difference in 8.7 fb^{-1} of 1.96 TeV data in the lepton+jets channel using a template methode to find $\Delta m_t = -1.95 \pm 1.11(stat.) \pm 0.59(syst.)$ GeV/c^2 [182] while DØ uses 3.6 fb^{-1} of lepton+jets events and the matrix element method with at least one b-tag. They find $\Delta m_t = 0.8 \pm 1.8(stat.) \pm 0.5(syst.)$ GeV/c^2 [183]. In 4.7 fb^{-1} of 7 TeV data, ATLAS measures the mass difference in lepton+jets events with a double b-tag requirement and hence very low background to find $\Delta m_t = 0.67 \pm 0.61(stat.) \pm 0.41(syst.)$ GeV/c^2 [184]. CMS measures the top-quark mass difference in 5 fb^{-1} of 7 TeV data in the lepton+jets channel and finds $\Delta m_t = -0.44 \pm 0.46(stat.) \pm 0.27(syst.)$ GeV/c^2 [185]. They repeat this measurement with 19.6 fb^{-1} of 8 TeV data to find $\Delta m_t = -0.15 \pm 0.19(stat.) \pm 0.09(syst.)$ GeV/c^2 [186]. All measurements are consistent with the SM expectation.

67.3.2.2. *Top-Quark Spin Correlations, Polarization, and Width:*

One of the unique features of the top quark is that it decays before its spin can be flipped by the strong interaction. Thus the top-quark polarization is directly observable via the angular distribution of its decay products. Hence, it is possible to define and measure observables sensitive to the top-quark spin and its production mechanism. Although the top- and antitop-quarks produced by strong interactions in hadron collisions are essentially unpolarized, the spins of t and $\bar{t}$ are correlated. For QCD production at threshold, the $t\bar{t}$ system is produced in a $^3S_1$ state with parallel spins for $q\bar{q}$ annihilation or in a $^1S_0$ state with antiparallel spins for gluon-gluon fusion. Hence, the situations at the Tevatron and at the LHC are somewhat complementary. However, at the LHC production of $t\bar{t}$ pairs at large invariant mass occurs primarily via fusion of gluons with opposite helicities, and the $t\bar{t}$ pairs so produced have parallel spins as in production at the Tevatron via $q\bar{q}$ annihilation. The direction of the top-quark spin is 100% correlated to the angular distributions of the down-type fermion (charged leptons or d-type quarks) in the decay. The joint angular distribution [187–189]

$$\frac{1}{\sigma}\frac{d^2\sigma}{d(\cos\theta_+)d(\cos\theta_-)} = \frac{1 + B_+\cos\theta_+ + B_-\cos\theta_- + \kappa\cdot\cos\theta_+\cdot\cos\theta_-}{4}, \qquad (67.4)$$

where θ_+ and θ_- are the angles of the daughters in the top-quark rest frame with respect to a particular spin quantization axis (assumed here to be the same for θ_+ and θ_-), is a very sensitive observable. The maximum value for κ, 0.782 at NLO at the Tevatron [190], is found in the off-diagonal basis [187], while at the LHC the value at NLO is 0.326 in the helicity basis [190]. The coefficients B_+ and B_- are near zero in the SM because the tops are unpolarized in $t\bar{t}$ production. In place of κ, $A\alpha_+\alpha_-$ is often used, where α_i is the spin analyzing power, and A is the spin correlation coefficient, defined as

$$A = \frac{N(\uparrow\uparrow) + N(\downarrow\downarrow) - N(\uparrow\downarrow) - N(\downarrow\uparrow)}{N(\uparrow\uparrow) + N(\downarrow\downarrow) + N(\uparrow\downarrow) + N(\downarrow\uparrow)}, \qquad (67.5)$$

where the first arrow represents the direction of the top-quark spin along a chosen quantization axis, and the second arrow represents the same for the antitop-quark. The spin analyzing power α_i is +0.998 for positively charged leptons, -0.966 for down-type quarks from W decays, and -0.393 for bottom quarks [191]. The sign of α flips for the respective antiparticles. The spin correlation could be modified by a new $t\bar{t}$ production mechanism such as through a Z' boson, Kaluza-Klein gluons, or a Higgs boson.

CDF used 5.1 fb^{-1} in the dilepton channel to measure the correlation coefficient in the beam axis [193]. The measurement was made using the expected distributions of $(\cos\theta_+, \cos\theta_-)$ and $(\cos\theta_b, \cos\theta_{\bar{b}})$ of the charged leptons or the b-quarks in the $t\bar{t}$ signal and background templates to calculate a likelihood of observed reconstructed distributions as a function of assumed κ. They determined the 68% confidence interval for the correlation coefficient κ as $-0.52 < \kappa < 0.61$ or $\kappa = 0.04 \pm 0.56$ assuming $m_t = 172.5$ GeV/c^2.

CDF also analyzed lepton+jets events in 5.3 fb^{-1} [194] assuming $m_t = 172.5$ GeV/c^2. They form three separate templates - the same-spin template, the opposite-spin template, and the background template for the 2-dimensional distributions in $\cos(\theta_l)\cos(\theta_d)$ vs. $\cos(\theta_l)\cos(\theta_b)$. The fit to the data in the helicity basis returns an opposite helicity fraction of $F_{OH} = 0.74 \pm 0.24(stat.) \pm 0.11(syst.)$. Converting this to the spin correlation coefficient yields $\kappa_{helicity} = 0.48 \pm 0.48(stat.) \pm 0.22(syst.)$. In the beamline basis, they find an opposite spin fraction of $F_{OS} = 0.86 \pm 0.32(stat.) \pm 0.13(syst.)$ which can be converted into a correlation coefficient of $\kappa_{beam} = 0.72 \pm 0.64(stat.) \pm 0.26(syst.)$.

DØ performed a measurement of the ratio f of events with correlated t and $\bar{t}$ spins to the total number of $t\bar{t}$ events in 5.3 fb^{-1} in the lepton+jets channel using a matrix element technique [195]. The SM expectation is $f = 1$. From 729 events, they obtain $f_{exp.} = 1.15^{+0.42}_{-0.43}(stat. + syst.)$ and can exclude values of $f < 0.420$ at the 95% C.L. In the dilepton channel [196], they also use a matrix element method and can exclude at the 97.7% C.L. the hypothesis that the spins of the t and $\bar{t}$ are uncorrelated. The combination [195] yields $f_{exp.} = 0.85 \pm 0.29$ $(stat + syst)$ and a $t\bar{t}$ production cross section which is in good agreement with the SM prediction and previous measurements. For an expected fraction of $f = 1$, they can exclude $f < 0.481$ at the 95% C.L. For the observed value of $f_{exp.} = 0.85$, they can exclude $f < 0.344(0.052)$ at the 95(99.7)% C.L. The observed fraction $f_{exp.}$ translates to a measured asymmetry value of $A_{exp.} = 0.66 \pm 0.23(stat. + syst.)$. They obtained the first evidence of SM spin correlation at 3.1 standard deviations.

Using 5.4 fb^{-1} of data, DØ measures the correlation in the dilepton channel also from the angles of the two leptons in the t and $\bar{t}$ rest frames, yielding a correlation strength $C = 0.10 \pm 0.45$ [197] (C is equivalent to negative κ in Eq. 4), in agreement with the NLO QCD prediction, but also in agreement with the no correlation hypothesis.

Spin correlations have been conclusively measured at the LHC by both the ATLAS and CMS collaborations. In the dominant gluon fusion production mode for $t\bar{t}$ pairs at the LHC, the angular distribution between the two leptons in $t\bar{t}$ decays to dileptons is sensitive to the degree of spin correlation [198].

The ATLAS collaboration has measured spin correlations in $t\bar{t}$ production at

$\sqrt{s} = 7$ TeV using 4.6 fb^{-1} of data. Candidate events are selected in the dilepton and lepton plus jets topologies. Four observables are used to extract the spin correlation: The difference, $\Delta\phi$ in azimuthal angle between the two charged leptons in dilepton events or the lepton and down-quark or bottom-quark candidate from the hadronic W-decay; An observable based on the ratio matrix elements with and without spin correlation; The double differential distribution of Eq. 4 in two different bases. The most sensitive measurement comes from using $\Delta\phi$ in dilepton events and results in $f_{\rm SM} = 1.19 \pm 0.09 \pm 0.18$. Using the helicity basis as the quantization axis, the strength of the spin correlation between the top- and antitop-quark is measured to be $A^{exp.}_{helicity} = 0.37 \pm 0.03 \pm 0.06$ [199], which is in agreement with the NLO prediction of about 0.31 [200]. Using the same events but converting $f_{exp.}$ into $A^{exp.}_{maximal}$ yields $A^{exp.}_{maximal} = 0.52 \pm 0.04 \pm 0.08$, to be compared to the NLO prediction of 0.44. In a similar analysis using 20.3 fb^{-1} of data at $\sqrt{s} = 8$ TeV, ATLAS measures $f_{\rm SM} = 1.20 \pm 0.05(stat.) \pm 0.13(syst.)$, corresponding to $A^{exp.}_{helicity} = 0.38 \pm 0.04$ [201], which compares well to the SM expectation of $A^{\rm SM}_{helicity} = 0.318 \pm 0.005$ [200]. ATLAS has released a measurement based on the correlation between the polar angles of the lepton in dilepton events [202]. The result, in the helicity basis, $A^{exp.}_{helicity} = 0.315 \pm 0.061 \pm 0.049$ is in good agreement with the SM prediction.

The CMS collaboration uses angular asymmetry variables in dilepton events, unfolded to the parton level. The most sensitive measurement is made using

$$A_{\Delta\phi} = \frac{N(\Delta\phi_{\ell^+\ell^-} > \pi/2) - N(\Delta\phi_{\ell^+\ell^-} < \pi/2)}{N(\Delta\phi_{\ell^+\ell^-} > \pi/2) + N(\Delta\phi_{\ell^+\ell^-} < \pi/2)}. \tag{67.6}$$

In 5.0 fb^{-1} of pp collisions at $\sqrt{s} = 7$ TeV, CMS measures $A_{\Delta\phi} = 0.113 \pm 0.010 \pm 0.006 \pm 0.012$ [203], where the uncertainties are statistical, systematic, and due to the reweighting of the top p_T in the Monte Carlo to match data.

Recent results from both CMS and ATLAS top spin measurements made at $\sqrt{s} = 8$ TeV. In 19.7 fb^{-1} of data, using a matrix element technique, CMS measures $f_{\rm SM} = 0.72 \pm 0.08^{+0.15}_{-0.13}$, corresponding to $A^{exp.}_{helicity} = 0.23 \pm 0.03^{+0.05}_{-0.04}$ [204]. Corresponding results obtained by studying the dilepton final state also show consistency with the SM expectations [192]. ATLAS has published an analysis of ten top-quark spin observables [205], corresponding to the coefficients in Eq. 4, and linear combinations thereof, measured in three different bases (including measuring the coefficient κ using a different basis for the top and anti-top decay products). The spin-correlation coefficient κ is measured in the helicity basis to be $\kappa = 0.296 \pm 0.093$ in good agreement with the SM expectation of 0.318. The polarization coefficients, B, in Eq. 4 are measured, also in the helicity basis, to be $B_+ = -0.044 \pm 0.038$ and $B_- = -0.064 \pm 0.040$, consistent with the SM predictions of 0.0030 ± 0.0010 and 0.0034 ± 0.00104, respectively.

ATLAS and CMS have also produced measurements of the polarization of top quarks in $t\bar{t}$ production at $\sqrt{s} = 7$ TeV. In 4.7 fb^{-1} of data, ATLAS measures the product of the leptonic spin-analyzing power (α_ℓ) and the top quark polarization. The measurement is made in one or two lepton final states, assuming that the polarization is introduced

by a CP-conserving (CPC) or maximally CP-violating (CPV) process. The results are $\alpha_\ell P_{CPC} = -0.035 \pm 0.014 \pm 0.037$ and $\alpha_\ell P_{CPV} = 0.020 \pm 0.016^{+0.013}_{-0.017}$ [206], where the uncertainties are statistical and systematic, respectively. The CMS measurement is made with 5.0 fb^{-1} of dilepton events. The polarization is extracted through an asymmetry, A_P, in the angular distribution of the two leptons, A_P, defined as

$$A_P = \frac{N(\cos\theta^*_\ell > 0) - N(\cos\theta^*_\ell < 0)}{N(\cos\theta^*_\ell > 0) + N(\cos\theta^*_\ell < 0)}, \tag{67.7}$$

where θ^* is the angle of the charged lepton in the rest frame of its parent top quark or antiquark. The polarization, P in the helicity basis is given by $P = 2A_P$. After unfolding to the parton level, the measurement yields $A_P = 0.005 \pm 0.013 \pm 0.014 \pm 0.008$ [203], where the uncertainties are, respectively, statistical, systematic, and from top-quark p_T reweighting. Both the ATLAS and CMS results are consistent with the SM expectation of negligible polarization.

A recent DØ publication [207] presents a measurement of top-quark polarization in $t\bar{t}$ production at the Tevatron. In 9.7 fb^{-1} of $p\bar{p}$ collisions, DØ uses lepton angular distributions in lepton+jets events to measure polarization in the beam, helicity, and transverse bases. The measurements are, respectively, 0.081 ± 0.048, -0.102 ± 0.061 and, 0.040 ± 0.035, where the beam-basis result is a combination with an earlier DØ result in dilepton events [208]. These results are all consistent near-zero polarization, as predicted in the SM.

Observation of top-quark spin correlations requires a top-quark lifetime less than the spin decorrelation timescale [209]. The top-quark width, inversely proportional to its lifetime, is expected to be of order 1 GeV/c^2 (Eq. 1). The sensitivity of current experiments does not approach this level in direct measurements. Nevertheless, several measurements have been made.

CDF presents a direct measurement of the top-quark width in the lepton+jets decay channel of $t\bar{t}$ events from a data sample corresponding to 8.7 fb^{-1} of integrated luminosity. The top-quark mass and the mass of the hadronically decaying W boson that comes from the top-quark decay are reconstructed for each event and compared with templates of different top-quark widths (Γ_t) and deviations from nominal jet energy scale (ΔJES) to perform a simultaneous fit for both parameters, where ΔJES is used for the *in situ* calibration of the jet energy scale. By applying a Feldman-Cousins approach, they establish an upper limit at 95% C.L. of $\Gamma_t < 6.38$ GeV and a two-sided 68% C.L. interval of 1.10 GeV $< \Gamma_t <$ 4.05 GeV, corresponding to a lifetime interval of $1.6 \times 10^{-15} < \tau_{top} < 6.0 \times 10^{-25}$ [210], consistent with the SM prediction. For comparison, a typical hadronization timescale is an order of magnitude larger than these limits. CMS uses partially reconstructed top-quarks in a clean sample of dilepton events to bound the top-quark width. In 12.9 fb^{-1} of data at $\sqrt{s} = 13$ TeV, CMS reports a 95% C.L. interval of $0.6 \leq \Gamma_t \leq 2.5$ GeV [211]. Recently ATLAS has provided a measurement by directly fitting reconstructed lepton+jets events in 20.2 fb^{-1} of data at $\sqrt{s} = 8$ TeV. They find $\Gamma_t = 1.76 \pm 0.33^{+0.79}_{-0.68}$ GeV [212].

The total width of the top-quark can also be determined from the partial decay width $\Gamma(t \to Wb)$ and the branching fraction $B(t \to Wb)$. DØ obtains $\Gamma(t \to Wb)$ from

the measured t-channel cross section for single top-quark production in 5.4 fb^{-1}, and $B(t \to Wb)$ is extracted from a measurement of the ratio $R = B(t \to Wb)/B(t \to Wq)$ in $t\bar{t}$ events in lepton+jets channels with 0, 1 and 2 b-tags. Assuming $B(t \to Wq) = 1$, where q includes any kinematically accessible quark, the result is: $\Gamma_t = 2.00^{+0.47}_{-0.43}$ GeV which translates to a top-quark lifetime of $\tau_t = (3.29^{+0.90}_{-0.63}) \times 10^{-25}$ s. Assuming a high mass fourth generation b' quark and unitarity of the four-generation quark-mixing matrix, they set the first upper limit on $|V_{tb'}| < 0.59$ at 95% C.L. [213]. A similar analysis has performed by CMS in 19.7 fb^{-1} of $\sqrt{s} = 8$ TeV data. It provides a better determination of the total width with respect to the measurement by DØ giving $\Gamma_t = 1.36 \pm 0.02(stat.)^{+0.14}_{-0.11}(syst.)$ GeV [214].

67.3.2.3. *W-Boson Helicity in Top-Quark Decay:*

The Standard Model dictates that the top quark has the same vector-minus-axial-vector $(V - A)$ charged-current weak interactions $\left(-i\frac{g}{\sqrt{2}}V_{tb}\gamma^{\mu}\frac{1}{2}(1-\gamma_5)\right)$ as all the other fermions. In the SM, the fraction of top-quark decays to longitudinally polarized W bosons is proportional to its Yukawa coupling and hence enhanced with respect to the weak coupling. It is expected to be [215] $\mathcal{F}_0^{\rm SM} \approx x/(1+x)$, $x = m_t^2/2M_W^2$ ($\mathcal{F}_0^{\rm SM} \sim 70\%$ for $m_t = 175$ GeV/c^2). Fractions of left-handed, right-handed, or longitudinal W bosons are denoted as $\mathcal{F}_-$, $\mathcal{F}_+$, and $\mathcal{F}_0$ respectively. In the SM, $\mathcal{F}_-$ is expected to be $\approx 30\%$ and $\mathcal{F}_+ \approx 0\%$. Predictions for the W polarization fractions at NNLO in QCD are available [216].

The Tevatron and the LHC experiments use various techniques to measure the helicity of the W boson in top-quark decays, in both the lepton+jets and in dilepton channels in $t\bar{t}$ production.

The first method uses a kinematic fit, similar to that used in the lepton+jets mass analyses, but with the top-quark mass constrained to a fixed value, to improve the reconstruction of final-state observables, and render the under-constrained dilepton channel solvable. Alternatively, in the dilepton channel the final-state momenta can also be obtained through an algebraic solution of the kinematics. The distribution of the helicity angle ($\cos\theta^*$) between the lepton and the b quark in the W rest frame provides the most direct measure of the W helicity. In a simplified version of this approach, the $\cos\theta^*$ distribution is reduced to a forward-backward asymmetry.

The second method (p_T^{ℓ}) uses the different lepton p_T spectra from longitudinally or transversely polarized W-decays to determine the relative contributions.

A third method uses the invariant mass of the lepton and the b-quark in top-quark decays ($M_{\ell b}^2$) as an observable, which is directly related to $\cos\theta^*$.

At the LHC, top-quark pairs in the dilepton channels are reconstructed by solving a set of six independent kinematic equations in the missing transverse energy in x- and in y-direction, two W-masses, and the two top/antitop-quark masses. In addition, the two jets with the largest p_T in the event are interpreted as b-jets. The pairing of the jets to the charged leptons is based on the minimization of the sum of invariant masses M_{min}. Simulations show that this criterion gives the correct pairing in 68% of the events.

Finally, the Matrix Element method (ME) has also been used, in which a likelihood is formed from a product of event probabilities calculated from the ME for a given set of measured kinematic variables and assumed W-helicity fractions.

The results of recent CDF, DØ, ATLAS, and CMS analyses are summarized in Table 67.2. The datasets are now large enough to allow for a simultaneous fit of $\mathcal{F}_0$, $\mathcal{F}_-$ and $\mathcal{F}_+$, which we denote by '3-param' or $\mathcal{F}_0$ and $\mathcal{F}_+$, which we denote by '2-param' in the table. Results with either $\mathcal{F}_0$ or $\mathcal{F}_+$ fixed at its SM value are denoted '1-param'. For the simultaneous fits, the correlation coefficient between the two values is about -0.8. A complete set of published results can be found in the Listings. All results are in agreement with the SM expectation.

CDF and DØ combined their results based on $2.7 - 5.4$ fb^{-1} [217] for a top-quark mass of 172.5 GeV/c^2. ATLAS presents results from 1.04 fb^{-1} of $\sqrt{s} = 7$ TeV data using a template method for the $\cos\theta^*$ distribution and angular asymmetries from the unfolded $\cos\theta^*$ distribution in the lepton+jets and the dilepton channel [219]. CMS performs a similar measurement based on template fits to the $\cos\theta^*$ distribution with 5.0 fb^{-1} of 7 TeV data in the lepton+jets final state [220]. As the polarization of the W bosons in top-quark decays is sensitive to the Wtb vertex Lorentz structure and anomalous couplings, both experiments also derive limits on anomalous contributions to the Wtb couplings. Recently, both experiments also combined their results from 7 TeV data to obtain values on the helicity fractions as well as limits on anomalous couplings [221].

At 8 TeV, ATLAS came out with a measurement of the W-helicity fractions in 20.2 fb^{-1} in lepton+jets events with at least one b-tag [222]. Using 19.8 fb^{-1} of 8 TeV data, CMS measured the W-helicity in lepton + 4 jet events with two b-tags [223]. In $t\bar{t}$ events with two opposite-sign leptons (electron or muon) in the final state in this dataset, CMS applied six kinematic constraints on the kinematics of the produced particles [224]. Also, using the same dataset a first measurement of the W-boson helicity in top-quark decays was made in electroweak single top production [225], yielding similarly precise and consistent results.

67.3.2.4. *Top-Quark Electroweak Charges:*

The top quark is the only quark whose electric charge has not been measured through production at threshold in e^+e^- collisions. Furthermore, it is the only quark whose electromagnetic coupling has not been observed and studied until recently. Since the CDF and DØ analyses on top-quark production did not associate the b, $\bar{b}$, and $W^\pm$ uniquely to the top or antitop, decays such as $t \to W^+\bar{b}, \bar{t} \to W^-b$ were not excluded. A charge 4/3 quark of this kind is consistent with current electroweak precision data. The $Z \to \ell^+\ell^-$ and $Z \to b\bar{b}$ data, in particular the discrepancy between A_{LR} from SLC at SLAC and $A_{FB}^{0,b}$ of b-quarks and $A_{FB}^{0,\ell}$ of leptons from LEP at CERN, can be fitted with a top quark of mass $m_t = 270$ GeV/c^2, provided that the right-handed b quark mixes with the isospin $+1/2$ component of an exotic doublet of charge $-1/3$ and $-4/3$ quarks, $(Q_1, Q_4)_R$ [226,227].

DØ studied the top-quark charge in double-tagged lepton+jets events, CDF did it in single tagged lepton+jets and dilepton events. Assuming the top- and antitop-quarks have equal but opposite electric charge, then reconstructing the charge of the b-quark

Table 67.2: Measurement and 95% C.L. upper limits of the W helicity in top-quark decays. The table includes both preliminary, as of September 2017, and published results. A full set of published results is given in the Listings.

W Helicity	Source	$\int \mathcal{L}dt$ (fb^{-1})	Ref.	Method
$\mathcal{F}_0 = 0.722 \pm 0.081$	CDF+DØ Run II	2.7-5.4	[217]	$\cos\theta^*$ 2-param
$\mathcal{F}_0 = 0.682 \pm 0.057$	CDF+DØ Run II	2.7-5.4	[217]	$\cos\theta^*$ 1-param
$\mathcal{F}_0 = 0.726 \pm 0.094$	CDF Run II	8.7	[218]	ME 2-param
$\mathcal{F}_0 = 0.67 \pm 0.07$	ATLAS (7 TeV)	1.0	[219]	$\cos\theta^*$ 3-param
$\mathcal{F}_0 = 0.682 \pm 0.045$	CMS (7 TeV)	5.0	[220]	$\cos\theta^*$ 3-param
$\mathcal{F}_0 = 0.626 \pm 0.059$	ATLAS+CMS (7 TeV)	2.2	[221]	$\cos\theta^*$ 3-param
$\mathcal{F}_0 = 0.709 \pm 0.019$	ATLAS (8 TeV)	20.2	[222]	$\cos\theta^*$ 3-param
$\mathcal{F}_0 = 0.681 \pm 0.026$	CMS (8 TeV)	19.8	[223]	$\cos\theta^*$ 3-param
$\mathcal{F}_0 = 0.653 \pm 0.029$	CMS (8 TeV)	19.7	[224]	$\cos\theta^*$ 3-param
$\mathcal{F}_0 = 0.720 \pm 0.054$	CMS (8 TeV)	19.7	[225]	$\cos\theta^*$ 3-param
$\mathcal{F}_+ = -0.033 \pm 0.046$	CDF+DØ Run II	2.7-5.4	[217]	$\cos\theta^*$ 2-param
$\mathcal{F}_+ = -0.015 \pm 0.035$	CDF+DØ Run II	2.7-5.4	[217]	$\cos\theta^*$ 1-param
$\mathcal{F}_+ = -0.045 \pm 0.073$	CDF Run II	8.7	[218]	ME 2-param
$\mathcal{F}_+ = 0.01 \pm 0.05$	ATLAS (7 TeV)	1.0	[219]	$\cos\theta^*$ 3-param
$\mathcal{F}_+ = 0.008 \pm 0.018$	CMS (7 TeV)	5.0	[220]	$\cos\theta^*$ 3-param
$\mathcal{F}_+ = 0.015 \pm 0.034$	ATLAS+CMS (7 TeV)	2.2	[221]	$\cos\theta^*$ 3-param
$\mathcal{F}_+ = -0.008 \pm 0.014$	ATLAS (8 TeV)	20.2	[222]	$\cos\theta^*$ 3-param
$\mathcal{F}_+ = -0.004 \pm 0.015$	CMS (8 TeV)	19.8	[223]	$\cos\theta^*$ 3-param
$\mathcal{F}_+ = 0.018 \pm 0.027$	CMS (8 TeV)	19.7	[224]	$\cos\theta^*$ 3-param
$\mathcal{F}_+ = -0.018 \pm 0.022$	CMS (8 TeV)	19.7	[225]	$\cos\theta^*$ 3-param

through jet charge discrimination techniques, the $|Q_{top}| = 4/3$ and $|Q_{top}| = 2/3$ scenarios can be differentiated. For the exotic model of Chang *et al.* [227] with a top-quark charge $|Q_{top}| = 4/3$, CDF excluded the model at 99% C.L. [228] in 5.6 fb^{-1}, while DØ excluded the model at a significance greater than 5 standard deviations using 5.3 fb^{-1} and set an upper limit of 0.46 on the fraction of such quarks in the selected sample [229]. These results indicate that the observed particle is indeed consistent with being a SM $|Q| = 2/3$ quark.

In 2.05 fb^{-1} at $\sqrt{s} = 7$ TeV, ATLAS performed a similar analysis, reconstructing the b-quark charge either via a jet-charge technique or via the lepton charge in soft muon decays in combination with a kinematic likelihood fit. They measure the top-quark charge

to be $0.64 \pm 0.02(stat.) \pm 0.08(syst.)$ from the charges of the top-quark decay products in single lepton $t\bar{t}$ events, and hence exclude the exotic scenario with charge $-4/3$ at more than 8σ [230].

In 4.6 fb^{-1} at $\sqrt{s} = 7$ TeV, CMS discriminates between the Standard Model and the exotic top-quark charge scenario in the muon+jets final states in $t\bar{t}$ events. They exploit the charge correlation between high-p_t muons from W-boson decays and soft muons from B-hadron decays in b-jets. Using an asymmetry technique, where $A = -1$ represent the exotic $Q = -4/3$ scenario and $A = +1$ the Standard Model $Q = +2/3$ scenario, they find $A_{meas} = 0.97 \pm 0.12(stat.) \pm 0.31(sys.)$, which agrees with the Standard Model expectation and excludes the exotic scenario at 99.9% C.L. [231].

The electromagnetic or the weak coupling of the top quark can be probed directly by investigating $t\bar{t}$ events with an additional gauge boson, such as $t\bar{t}\gamma$, $t\bar{t}W$, and $t\bar{t}Z$ events.

CDF performed a search for events containing a lepton, a photon, significant missing transverse momentum, and a jet identified as containing a b-quark and at least three jets and large total transverse energy in 6.0 fb^{-1}. They reported evidence for the observation of $t\bar{t}\gamma$ production with a cross section $\sigma_{t\bar{t}\gamma} = 0.18 \pm 0.08$ pb and a ratio of $\sigma_{t\bar{t}\gamma}/\sigma_{t\bar{t}} = 0.024 \pm 0.009$ [232].

ATLAS performed a first measurement of the $t\bar{t}\gamma$ cross section in pp collisions at $\sqrt{s} = 7$ TeV using 4.6 fb^{-1} of data. Events are selected that contain a large transverse momentum electron or muon and a large transverse momentum photon, yielding 140 and 222 events in the electron and muon samples, respectively. The production of $t\bar{t}\gamma$ events was observed with a significance of 5.3% standard deviations. The resulting cross section times branching ratio into the single lepton channel for $t\bar{t}\gamma$ production with a photon with transverse momentum above 20 GeV is $\sigma^{fid.}(t\bar{t}\gamma) \times BR = 63 \pm 8(stat.)^{+17}_{-13}(syst.) \pm 1(lumi.)$ pb per lepton flavour [233], which is consistent with leading-order theoretical calculations. Using 19.7 fb^{-1} of data at 8 TeV, CMS performed a similar measurement of the $t\bar{t}\gamma$ production cross section in the lepton+jets decay mode with a photon transverse momentum above 25 GeV and $|\eta|$ <1.44. They obtain a normalized cross section $\mathcal{R} = \sigma_{t\bar{t}+\gamma}/\sigma_{t\bar{t}} = (5.7 \pm 1.8) \times 10^{-4}$ in e+jets and $(4.7 \pm 1.3) \times 10^{-4}$ in μ+jets. The fiducial $t\bar{t}\gamma$ cross section is obtained by multiplying by the measured $t\bar{t}$ fiducial cross section of $244.9 \pm 1.4(stat.)^{+6.3}_{-5.5}(sys.) \pm 6.4(lumi.)$pb. Extrapolating to the full phase space, the result is $\sigma_{t\bar{t}\gamma}\times$BR=$(515 \pm 108)$ fb, per lepton+jets final state [234], in good agreement with the theoretical prediction. Also at 8 TeV, ATLAS has used 20.2 fb^{-1} of data to measure the $t\bar{t}\gamma$ cross section with a photon above 15 GeV and $|\eta| < 2.37$. The fiducial cross section is measured to be 139 ± 18 fb [235], in good agreement with the NLO prediction. A precision test of the vector and axial vector couplings in $t\bar{t}\gamma$ events or searches for possible tensor couplings of top-quarks to photons will only be feasible with an integrated luminosity of several hundred fb^{-1} in the future.

ATLAS and CMS have also studied the associate production of top-antitop quark pairs along with an electroweak gauge boson, where in the Standard Model the W-boson is expected to be produced via initial state radiation, while the Z-boson can also be radiated from a final-state top-quark and hence provides sensitivity to the top-quark

neutral current weak gauge coupling, which implies a sensitivity to the third component of the top-quark's weak isospin.

CMS performed measurements of the $t\bar{t}W$ and $t\bar{t}Z$ production cross section at $\sqrt{s} = 7$ TeV with 5 fb^{-1}, yielding results at about 3 standard deviations significance [236]. ATLAS performed a similar analysis with 4.7 fb^{-1} in the three-lepton channel and set an upper limit of 0.71 pb at 95% C.L. [237].

Using 20.3 fb^{-1} of 8 TeV data, ATLAS performs a simultaneous measurement of the $t\bar{t}W$ and $t\bar{t}Z$ cross section. They observe the $t\bar{t}W$ and $t\bar{t}Z$ production at the 5.0σ and 4.2σ level, respectively, yielding $\sigma_{t\bar{t}W} = 369^{+100}_{-91}$ fb and $\sigma_{t\bar{t}Z} = 176^{+58}_{-52}$ fb [238]. CMS performs an analysis where signal events are identified by matching reconstructed objects in the detector to specific final state particles from $t\bar{t}W$ and $t\bar{t}Z$ decays. using 19.5 fb^{-1} of 8 TeV data. They obtain $\sigma_{t\bar{t}W} = 382^{+117}_{-102}$ fb and $\sigma_{t\bar{t}Z} = 242^{+65}_{-55}$ fb, yielding a significance of 4.8 and 6.4 standard, respectively [239]. These measurements are used to set bounds on five anomalous dimension-six operators that would affect the $t\bar{t}W$ and $t\bar{t}Z$ cross sections.

The most recent measurements in these channels are made at 13 TeV from ATLAS and CMS in multilepton final states. Using 3.2 fb^{-1} of data, ATLAS has made measurements of the $t\bar{t}W$ and $t\bar{t}Z$ cross sections in multilepton final states. Using a likelihood technique to fit signal and control regions, ATLAS measured $t\bar{t}W$ and $t\bar{t}Z$ production cross sections of 1.5 ± 0.8 pb and 0.9 ± 0.3 pb, and significances over the background-only hypotheses of 2.2σ and 3.9σ, respectively [240]. The results are consistent with Standard Model expectations. CMS uses 35.9 fb^{-1} of data to measure $t\bar{t}W$ and $t\bar{t}Z$ production cross sections of $0.80^{+0.12\ +0.13}_{-0.11\ -0.12}$ pb and $1.00^{+0.09\ +0.12}_{-0.08\ -0.10}$ pb, and significances over the background-only hypotheses of 5.5σ and 9.5σ, respectively [241], firmly establishing the observation of these processes.

The electroweak couplings can also be probed in single-top production in association with a Z boson. The $pp \to tZq$ process at the LHC probes both the WWZ coupling in the case where the Z emerges from the t-channel W in single-top production and, in the case where the Z is radiated from the top quark, the tZ coupling. A CMS search at 8 TeV produced a hint of a tZq signal in tri-lepton events, with a significance compared to the background-only hypothesis of 2.4σ [242]. At 13 TeV the signal has begun to emerge. ATLAS uses 36.1 fb^{-1} of 13 TeV data in events with three leptons and two jets, at least one of which is b-tagged, to extract with a neural-network technique, a tZq cross section of $600 \pm 170 \pm 140$ fb, with a significance of 4.2σ [243]. The result is in agreement with the Standard Model NLO calculation, which predicts a production cross section of 800 fb. In the same final state, and with a BDT analysis, CMS uses 35.9 fb^{-1} of 13 TeV data to measure $\sigma(pp \to tZq \to Wb\ell^+\ell^- q) = 123^{+44}_{-39}$fb, where the leptons include electrons, muons, and taus [244]. The observed significance is 3.7σ.

67.3.3. ***Searches for Physics Beyond the Standard Model*** :

The top quark plays a special role in the SM. Being the only quark with a coupling to the Higgs boson of order one, it provides the most important contributions to the quadratic radiative corrections to the Higgs mass exposing the issue of the naturalness of the SM. It is therefore very common for models where the naturalness problem is addressed to have new physics associated with the top quark. In SUSY, for instance, naturalness predicts the scalar top partners to be the lightest among the squarks and to be accessible at the LHC energies (see the review "Supersymmetry: Theory"). In models where the Higgs is a pseudo-Goldstone boson, such as Little Higgs models, naturalness predicts the existence of partners of the top quarks with the same spin and color, but with different electroweak couplings, the so-called vectorial t'. Stops and t''s are expected to have sizable branching ratios to top quarks. Another intriguing prediction of SUSY models with universal couplings at the unification scale is that for a top-quark mass close to the measured value, the running of the Yukawa coupling down to 1 TeV naturally leads to the radiative breaking of the electroweak symmetry [245]. In fact, the top quark plays a role in the dynamics of electroweak symmetry breaking in many models [246]. One example is topcolor [247], where a large top-quark mass can be generated through the formation of a dynamic $t\bar{t}$ condensate, X, which is formed by a new strong gauge force coupling preferentially to the third generation. Another example is topcolor-assisted technicolor [248], predicting the existence of a heavy Z' boson that couples preferentially to the third generation of quarks. If light enough such a state might be directly accessible at the present hadron collider energies, or if too heavy, lead to four-top interactions possibly visible in the $t\bar{t}t\bar{t}$ final state, for which limits on production cross sections at the LHC $\sqrt{s} = 8$ and 13 TeV exist [249–252].

Current strategies to search for new physics in top-quark events at hadron colliders are either tailored to the discovery of specific models or model independent. They can be broadly divided in two classes. In the first class new resonant states are looked for through decay processes involving the top quarks. Current searches for bosonic resonances in $t\bar{t}$ final states, or for direct stop and t' production, or for a charged Higgs in $H^+ \to t\bar{b}$ fall in the category. On the other hand, if new states are too heavy to be directly produced, they might still give rise to deviations from the SM predictions for the strength and Lorentz form of the top-quark couplings to other SM particles. Accurate predictions and measurements are therefore needed and the results be efficiently systematized in the framework of an effective field theory [253,254]. For instance, the efforts to constrain the structure of the top couplings to vector bosons (g, γ, Z, W) and to the Higgs boson, including flavor-changing neutral currents involving the top quark, fall in this second category.

67.3.3.1. *New Physics in Top-Quark Production:*

Theoretical [255–256] and experimental efforts have been devoted to the searches of $t\bar{t}$ resonances.

At the Tevatron, both the CDF and DØ collaborations have searched for resonant production of $t\bar{t}$ pairs in the lepton+jets channel [257,258]. In both analyses, the data indicate no evidence of resonant production of $t\bar{t}$ pairs. They place upper limits on the production cross section times branching fraction to $t\bar{t}$ in comparison to the prediction for a narrow ($\Gamma_{Z'} = 0.012 M_{Z'}$) leptophobic topcolor Z' boson. Within this model, they exclude Z' bosons with masses below 915 (CDF-full data set) and 835 (DØ, 5 fb^{-1}) GeV/c^2 at the 95% C.L. These limits turn out to be independent of couplings of the $t\bar{t}$ resonance (pure vector, pure axial-vector, or SM-like Z'). A similar analysis has been performed by CDF in the all-jets channel using 2.8 fb^{-1} of data [259].

At the LHC, both the CMS and ATLAS collaborations have searched for resonant production of $t\bar{t}$ pairs, employing different techniques and final-state signatures (all-jets, lepton+jets, dilepton) at $\sqrt{s}$ = 7, 8 and 13 TeV. In the low mass range, from the $t\bar{t}$ threshold to about one TeV, standard techniques based on the reconstruction of each of the decay objects (lepton, jets and b-jets, missing E_T) are used to identify the top quarks, while at higher invariant mass, the top quarks are boosted and the decay products more collimated and can appear as large-radius jets with substructure. Dedicated reconstruction techniques have been developed in recent years for boosted top quarks [260] that are currently employed at the LHC. Most of the analyses are model-independent (i.e., no assumption on the quantum numbers of the resonance is made) yet they assume a small width and no signal-background interference.

Using lepton+jets and fully hadronic channels in a data set corresponding to an integrated luminosity of 2.6 fb^{-1} at 13 TeV, the CMS collaboration finds no significant deviations from the SM background [261] and improves the limits obtained at 8 TeV for resonances with masses above 2 TeV/c^2. In particular, the existence of a leptophobic topcolor particle Z' is excluded at the 95% confidence level for resonances in the mass range $0.6 < M_{Z'} < 2.5$ TeV/c^2, $0.5 < M_{Z'} < 3.9$ TeV/c^2, and $0.5 < M_{Z'} < 4.0$ TeV/c^2 for $\Gamma_{Z'} = 1\%, 10\%, 30\% M_{Z'}$, respectively [261]. Kaluza-Klein excitations of a gluon with masses between $0.5 < M_{G_{KK}} < 3.3$ TeV/c^2 (at 95% confidence level) in the Randall-Sundrum model are also excluded.

The ATLAS collaboration has performed a search for resonant $t\bar{t}$ production in the lepton+jets channel using 4.7 fb^{-1} (20.3 fb^{-1}) of proton-proton (pp) collision data collected at a center-of-mass energy $\sqrt{s}$ = 7(8) TeV [262,263]. The $t\bar{t}$ system is reconstructed using both small-radius and large-radius jets, the latter being supplemented by a jet substructure analysis. A search for local excesses in the number of data events compared to the Standard Model expectation in the $t\bar{t}$ invariant mass spectrum is performed. No evidence for a $t\bar{t}$ resonance is found and 95% confidence-level limits on the production rate are determined for massive states predicted in two benchmark models. The most stringent limits come from the sample collected at 8 TeV. The upper limits on the cross section times branching ratio of a narrow Z' boson decaying to top-quark pairs range from 4.2 pb for a resonance mass of 0.4 TeV/c^2 to 0.03 pb for a mass of 3 TeV/c^2. A narrow leptophobic topcolor Z' boson with a mass below 1.8 TeV/c^2 is

excluded. Upper limits are set on the cross section times branching ratio for a broad color-octet resonance with $\Gamma/m = 15\%$ decaying to $t\bar{t}$. These range from 2.5 pb for a mass of 0.4 TeV/c^2 to 0.03 pb for a mass of 3 TeV/c^2. A Kaluza-Klein excitation of the gluon in a Randall-Sundrum model (a slightly different model is used compared to CMS) is excluded for masses below 2.2 TeV/c^2.

ATLAS has also conducted a search in the all-jet final state at 7 TeV corresponding to an integrated luminosity of 4.7 fb^{-1} [264]. The $t\bar{t}$ events are reconstructed by selecting two top quarks in their fully hadronic decay modes which are reconstructed using the Cambridge/Aachen jet finder algorithm with a radius parameter of 1.5. The substructure of the jets is analysed using the HEPTopTagger algorithm [265] to separate top-quark jets from those originating from gluons and lighter quark jets. The invariant mass spectrum of the data is compared to the SM prediction, and no evidence for resonant production of top-quark pairs is found. The data are used to set upper limits on the cross section times branching ratio for resonant $t\bar{t}$ production in two models at 95% confidence level. Leptophobic Z' bosons with masses between 700 and 1000 GeV/c^2 as well as $1280 - 1320$ GeV/c^2 and Kaluza-Klein-Gluons with masses between 700 and 1620 GeV/c^2 are excluded at the 95% confidence level.

Heavy charged bosons, such as W' or H^+, can also be searched for in $t\bar{b}, tj$ final states (for more information see the review "W'-boson searches" and "Higgs Bosons: theory and searches"), while heavy fermion resonances, such as vectorial or excited quarks, in final states such as tZ, tH, tW, bW.

CMS has performed several searches in this context, the most stringent limits coming from those at at $\sqrt{s} = 13$ TeV [266–272]. For instance, a $W' \to t\bar{b}$ has been searched for in both lepton+jets in 35.9 fb^{-1}. No evidence has been found for a right-handed W' boson and masses below 3.6 TeV/c^2 are excluded at 95% confidence level providing the most stringent limits for right-handed W' bosons in the top and bottom quark decay channel to date [266]. Single production of a vector-like quark T decaying to a Z boson and a top quark, with the Z boson decaying leptonically and the top quark decaying hadronically, has also been searched for in the same data set. At the 95% confidence level, the product of cross section and branching fraction has been excluded above values in the range 0.27-0.04 pb for vector-like quark masses in the range 0.7-1.7 TeV/c^2. In the same selection, the production of a heavy Z' boson decaying to Tt, with T decaying to tZ, has been also searched for and limits on the product of cross section and branching fractions for this process are set between 0.13 and 0.06 pb for Z' boson masses in the range from 1.5 to 2.5 TeV/c^2 [267]. Finally, a search for the production of heavy partners of the top quark with charge 5/3 decaying into a top quark and a W boson has been performed with a data sample corresponding to an integrated luminosity of 2.3 fb^{-1}, considering final states with either a pair of same-sign leptons or a single lepton plus jets. In absence of an excess, a 5/3 charged top quark with right-handed (left-handed) couplings has been excluded at 95% confidence level for masses below 1020 (990) GeV [268].

ATLAS has performed searches for heavy bosons and fermions decaying to one top quark at $\sqrt{s} = 7$ and 8 TeV. For example, t-jet resonances have been searched in the lepton+jets channel of $t\bar{t}$+ jets events in 4.7 fb^{-1} at $\sqrt{s} = 7$ TeV [273]. A heavy new particle, assumed to be produced singly in association with a $t(\bar{t})$ quark, decays

to a $t(\bar{t})$ quark and a light flavor quark, leading to a color singlet (triplet) resonance in the $t(\bar{t})$+jet system. The full 2011 ATLAS pp collision dataset from the LHC (4.7 fb^{-1}) is used to select $t\bar{t}$ events. The data are consistent with the SM expectation and a new particle with mass below 350 (430) GeV/c^2 for W (color triplet) models is excluded with a 95% confidence level, assuming unit right-handed coupling. ATLAS has conducted a search for the single and pair production of a new charge +2/3 quark (T) decaying via $T \to Zt$ (and also -1/3 quark (B) decaying via $B \to Zb$) in a dataset corresponding to 20.3 fb^{-1} luminosity at $\sqrt{s} = 8$ TeV [274]. Selected events contain a high transverse momentum Z-boson candidate reconstructed from a pair of oppositely charged electrons or muons. Additionally, the presence of at least two jets possessing properties consistent with the decay of a b-hadron is required, as well as large total transverse momentum of all central jets in the event. No significant excess of events above the SM expectation is observed, and upper limits are derived for vector-like quarks of various masses in a two-dimensional plane of branching ratios. Under branching ratio assumptions corresponding to a weak-isospin singlet scenario, a T quark with mass lower than 655 GeV/c^2 is excluded at the 95% confidence level. Under branching ratio assumptions corresponding to a particular weak-isospin doublet scenario, a T quark with mass lower than 735 GeV/c^2 is excluded at the 95% confidence level.

A complementary search performed by ATLAS in the lepton+jets final state of the same dataset [250], characterized by an isolated electron or muon with moderately high transverse momentum, significant missing transverse momentum, and multiple jets is performed to look for $T(B) \to Wb, Zt, Ht(Wt, Zb, Hb)$ decays. No significant excess of events above the SM expectation is observed, and upper limits are derived for vector-like quarks of various masses under several branching ratio hypotheses. The 95% C.L. observed lower limits on the T quark mass range between 715 GeV and 950 GeV for all possible values of the branching ratios into the three decay modes. In addition this study provides limits on four top-quark production and production of two positively-charged top quarks. No significant excess of events over the background expectation is observed. The four top-quark production cross section must be less than 23 fb in the SM and less than 12 fb for production via a contact interaction; in the case of sgluon pair production decaying to $t\bar{t}$, where a sgluon is a scalar partner of the gluino [275], the mass of a sgluon must be greater than 1.06 TeV/c^2. Finally, limits in the context of models featuring two extra dimensions are also set.

In many models top-quark partners preferably decay to top quarks and weakly interacting neutral stable particles, i.e., possibly dark matter candidates, that are not detected. An observable especially sensitive to new physics effects in $t\bar{t}$ production is therefore the missing momentum.

CMS has presented a differential cross section measurement of top-quark pair production with missing transverse energy and corresponding interpretations in the context of dark matter (effective and simplified) models at 8 and 13 TeV [276–278]. The results obtained so far are consistent with the SM expectations. In particular the search performed at 13 TeV [278] is based on 2.2 fb^{-1} of integrated luminosity and include double-leptonic, single-lepton and all-jet final states. Upper limits are derived on the production cross section and interpreted in terms of a simplified model with

a scalar/pseudoscalar mediator. Cross sections larger than 1.5 (1.8) times the values predicted for a 10 GeV scalar (pseudoscalar) mediator, respectively, for couplings of $g_q = g_c = 1$ are excluded at 95% C.L.

An analogous search, at a center-of-mass energy of 7 TeV in 1.04 fb^{-1} of data has been performed by ATLAS [279]. The search is carried out in the lepton+jets channel. The results are interpreted in terms of a model where new top-quark partners are pair-produced and each decay to an on-shell top (or antitop) quark and a long-lived undetected neutral particle. The data are found to be consistent with SM expectations. A limit at 95% C.L. is set excluding a cross-section times branching ratio of 1.1 pb for a top-partner mass of 420 GeV/c^2 and a neutral particle mass less than 10 GeV/c^2. In a model of exotic fourth generation quarks, top-partner masses are excluded up to 420 GeV/c^2 and neutral particle masses up to 140 GeV/c^2.

Flavor-changing-neutral-currents (FCNC) are hugely suppressed in the SM as non zero contributions only arise at one-loop and are proportional to the splitting between the quark masses. In the case of the top quark $B(t \to Bq)$ with $B = g, \gamma, Z, H$ and $q = u, c$ are predicted to be order of 10^{-12} ($t \to cg$) or much smaller [280]. Several observables are accessible at colliders to test and constrain such couplings.

CMS has performed several studies on the search for FCNC in top-quark production. They have considered single top quark production in the t-channel in 5 fb^{-1} integrated luminosity at 7 TeV and 19.7 fb^{-1} integrated luminosity at 8 TeV [281]. Events with the top quark decaying into a muon, neutrino and two or three jets are selected. The upper limits on effective coupling strength can be translated to the 95% upper limits on the corresponding branching ratios $B(t \to gu) \leq 2.0 \cdot 10^{-5}$, $B(t \to gc) \leq 4.1 \cdot 10^{-4}$. They have performed a search for a single top quark produced in association with a photon in 19.1 fb^{-1} integrated luminosity at 8 TeV [282]. The event selection requires the presence of one isolated muon and jets in the final state. The upper limits on effective coupling strength can be translated to the 95% upper limits on the corresponding branching ratios $B(t \to \gamma u) \leq 0.0161\%$, $B(t \to \gamma c) \leq 0.182\%$.

Recently, a search for flavor-changing neutral currents in associated production of a top quark with a Higgs boson decaying into $b\bar{b}$ has also been presented by CMS, corresponding to an integrated luminosity of 35.9 fb^{-1} at 13 TeV. Two complementary channels are considered: top quark pair production, with FCNC decay of the top quark or antiquark, and single top associated production. A final state with one isolated lepton and at least three reconstructed jets, among which at least two are identified as b quark jets, is considered. No significant deviation is observed from predicted background and upper limits at 95% confidence level are set on the branching ratios of top quark decays, $B(t \to uH) < 0.47\%$ and $B(t \to cH) < 0.47\%$ [283], which are similar to the combined limits on all decay channels obtained with the full data set at 8 TeV [284].

ATLAS has presented results on the search for single top-quark production via FCNC's in strong interactions using data collected at $\sqrt{s}$=8 TeV and corresponding to an integrated luminosity of 20.3 fb^{-1}. Flavor-changing-neutral-current events are searched for in which a light quark (u or c) interacts with a gluon to produce a single top quark, either with or without the associated production of another light quark or gluon. Candidate events of top quarks decaying into leptons and jets are selected and classified

into signal- and background-like events using a neural network. The observed 95% C.L. limit is $\sigma_{qq\to t} \times B(t \to Wb) < 3.4$ pb that can be interpreted as limits on the branching ratios, $B(t \to ug) < 4 \cdot 10^{-5}$ and $B(t \to cg) < 1.7 \cdot 10^{-4}$ [285]. This result supersedes the corresponding 7 TeV analysis in 2 fb^{-1} [286].

Constraints on FCNC couplings of the top quark can also be obtained from searches for anomalous single top-quark production in e^+e^- collisions, via the process $e^+e^- \to \gamma, Z^* \to t\overline{q}$ and its charge-conjugate ($q = u, c$), or in $e^{\pm}p$ collisions, via the process $e^{\pm}u \to e^{\pm}t$. For a leptonic W decay, the topology is at least a high-p_T lepton, a high-p_T jet and missing E_T, while for a hadronic W-decay, the topology is three high-p_T jets. Limits on the cross section for this reaction have been obtained by the LEP collaborations [287] in e^+e^- collisions, and by H1 [288] and ZEUS [289] in $e^{\pm}p$ collisions. When interpreted in terms of branching ratios in top decay [290,291], the LEP limits lead to typical 95% C.L. upper bounds of $B(t \to qZ) < 0.137$. Assuming no coupling to the Z boson, the 95% C.L. limits on the anomalous FCNC coupling $\kappa_\gamma < 0.13$ and < 0.27 by ZEUS and H1, respectively, are stronger than the CDF limit of $\kappa_\gamma < 0.42$, and improve over LEP sensitivity in that domain. The H1 limit is slightly weaker than the ZEUS limit due to an observed excess of five-candidate events over an expected background of 3.2 ± 0.4. If this excess is attributed to FCNC top-quark production, this leads to a total cross section of $\sigma(ep \to e + t + X, \sqrt{s} = 319 \text{ GeV}) < 0.25$ pb [288,292].

67.3.3.2. *New Physics in Top-Quark decays:*

The large sample of top quarks produced at the Tevatron and the LHC allows to measure or set stringent limits on the branching ratios of rare top-quark decays. For example, the existence of a light H^+ can be constrained by looking for $t \to H^+b$ decay, in particular with tau-leptons in the final state (for more information see the review "Higgs Bosons: theory and searches").

A first class of searches for new physics focuses on the structure of the Wtb vertex. Using up to 2.7 fb^{-1} of data, DØ has measured the Wtb coupling form factors by combining information from the W-boson helicity in top-quark decays in $t\bar{t}$ events and single top-quark production, allowing to place limits on the left-handed and right-handed vector and tensor couplings [293–295].

ATLAS has published the results of a search for CP violation in the decay of single top quarks produced in the t-channel where the top quarks are predicted to be highly polarized, using the lepton+jets final state [296]. The data analyzed are from pp collisions at $\sqrt{s} = 7$ TeV and correspond to an integrated luminosity of 4.7 fb^{-1}. In the Standard Model, the couplings at the Wtb vertex are left-handed, right-handed couplings being absent. A forward-backward asymmetry with respect to the normal to the plane defined by the W-momentum and the top-quark polarization has been used to probe the complex phase of a possibly non-zero value of the right-handed coupling, signaling a source of CP-violation beyond the SM. The measured value of the asymmetry is $0.031 \pm 0.065(stat.)^{+0.029}_{-0.031}(syst.)$ in good agreement with the Standard Model.

A second class of searches focuses on FCNC's in the top-quark decays. Both, CDF and DØ, have provided the first limits for FCNC's in Run I and II. The most recent results from CDF give $B(t \to qZ) < 3.7\%$ and $B(t \to q\gamma) < 3.2\%$ at the 95%

C.L. [297] while DØ [298,299] sets $B(t \to qZ)(q = u, c \text{ quarks }) < 3.2\%)$ at 95% C.L., $B(t \to gu) < 2.0 \cdot 10^{-4}$, and $B(t \to gc) < 3.9 \cdot 10^{-3}$ at the 95% C.L.

At the LHC, CMS has used a sample at a center-of-mass energy of 8 TeV corresponding to 19.7 fb^{-1} of integrated luminosity to perform a search for flavor changing neutral current top-quark decay $t \to Zq$. Events with a topology compatible with the decay chain $t\bar{t} \to Wb + Zq \to \ell\nu\ b + \ell\ell q$ are searched for. There is no excess seen in the observed number of events relative to the SM prediction; thus no evidence for flavor changing neutral current in top-quark decays is found. A combination with a previous search at 7 TeV excludes a $t \to Zq$ branching fraction greater than 0.05% at the 95% confidence level [300]. CMS has also performed a search for the production of a single top quark in association with a Z boson in the same data set at 8 TeV. Final states with three leptons (electrons or muons) and at least one jet are investigated. Exclusion limits at 95% confidence level on the branching fractions are found to be $B(t \to uZ) < 0.022\%$ and $B(t \to cZ) < 0.049\%$ [301].

The ATLAS collaboration has also searched for FCNC processes in 20.3 fb^{-1} of $t\bar{t}$ events with one top quark decaying through FCNC ($t \to qZ$) and the other through the SM dominant mode ($t \to bW$). Only the decays of the Z boson to charged leptons and leptonic W boson decays were considered as signal, leading to a final state topology characterized by the presence of three isolated leptons, at least two jets and missing transverse energy from the undetected neutrino. No evidence for an FCNC signal was found. An upper limit on the $t \to qZ$ branching ratio of $B(t \to qZ) < 7 \times 10^{-4}$ is set at the 95% confidence level [302], which supersedes previous results [303].

Another search for FCNCs is in the decay of a top-quark to a Higgs boson plus a light parton, $t \to qH$, $q = u, c$. The CMS collaboration has performed two searches using a sample at a center-of-mass energy of 8 TeV corresponding to 19.7 fb^{-1} of integrated luminosity, combining multi-lepton, $\gamma\gamma$ and $b\bar{b}$ final states [284]. The combined analysis sets an upper limit on the $t \to c(u)H$ branching ratios of $B(t \to c(u)H) < 0.40(0.55)\%$ at 95% confidence level. The ATLAS collaboration considers $t \to qH$, $q = u, c$ with 4.7 fb^{-1} of $t\bar{t}$ events at $\sqrt{s} = 7$ TeV and 20.3 fb^{-1} of $t\bar{t}$ events at $\sqrt{s} = 8$ TeV. A combined measurement including $H \to \gamma\gamma$ and $H \to WW*, \tau\tau$ modes yields a 95% C.L. upper limit of 0.46% and 0.45% on the branching ratios of $B(t \to cH)$ and $B(t \to uH)$, respectively [304].

67.4. Outlook

Top-quark physics at hadron colliders has developed into precision physics. Various properties of the top quark have been measured with high precision, where the LHC is about to or has already reached the precision of the Tevatron. Several $\sqrt{s}$-dependent physics quantities, such as the production cross-section, have been measured at several energies at the Tevatron and the LHC. Up to now, all measurements are consistent with the SM predictions and allow stringent tests of the underlying production mechanisms by strong and weak interactions. Given the very large event samples available at the LHC, top-quark properties will be further determined in $t\bar{t}$ as well as in electroweak single top-quark production. At the Tevatron, the $t-$ and $s-$channels for electroweak

single top-quark production have been measured separately. At the LHC, significant progress has been achieved and all the three relevant channels are expected to be independently accessible in the near future. Furthermore, $t\bar{t}\gamma$, $t\bar{t}Z$, and $t\bar{t}W$ together with $t\bar{t}H$ associated production have started to or will provide further information on the top-quark electroweak couplings. At the same time various models of physics beyond the SM involving top-quark production are being constrained. With the first results from LHC Run-II at a higher center-of-mass energy and much higher luminosity starting to be released, top-quark physics has the potential to shed light on open questions and new aspects of physics at the TeV scale.

CDF note references can be retrieved from
`www-cdf.fnal.gov/physics/new/top/top.html`,
and DØ note references from `www-d0.fnal.gov/Run2Physics/WWW/documents/Run2Results.htm` ,
and ATLAS note references from `https://twiki.cern.ch/twiki/bin/view/AtlasPublic/TopPublicResults` ,
and CMS note references from `https://twiki.cern.ch/twiki/bin/view/CMSPublic/PhysicsResultsTOP`.

References:

1. M. Czakon, P. Fiedler, and A. Mitov, Phys. Rev. Lett. **110**, 252004 (2013).
2. ATLAS, CMS, CDF, & DØ Collabs., `arXiv:1403.4427`.
3. S. Cortese and R. Petronzio, Phys. Lett. **B253**, 494 (1991).
4. S. Willenbrock and D. Dicus, Phys. Rev. **D34**, 155 (1986).
5. N. Kidonakis, Phys. Rev. **D83**, 091503 (2011).
6. M. Brucherseifer, F. Caola, and K. Melnikov, Phys. Lett. **B736**, 58 (2014).
7. E. Berger, J. Gao, H. Xing Zhu, `arXiv:1708.09405`.
8. N. Kidonakis, Phys. Rev. **D81**, 054028 (2010).
9. N. Kidonakis, Phys. Rev. **D82**, 054018 (2010).
10. T. Tait and C.-P. Yuan. Phys. Rev. **D63**, 014018 (2001).
11. M. Jeżabek and J.H. Kühn, Nucl. Phys. **B314**, 1 (1989).
12. I.I.Y. Bigi *et al.*, Phys. Lett. **B181**, 157 (1986).
13. A.H. Hoang *et al.*, Phys. Rev. **D65**, 014014 (2002).
14. K. Hagiwara, Y. Sumino, and H. Yokoya, Phys. Lett. **B666**, 71 (2008).
15. A. Czarnecki and K. Melnikov, Nucl. Phys. **B544**, 520 (1999); K.G. Chetyrkin *et al.*, Phys. Rev. **D60**, 114015 (1999).
16. S. Frixione, P. Nason, and B. Webber, JHEP **08**, 007 (2003); S. Frixione, P. Nason, and C. Oleari, JHEP **07**, 070 (2007); S. Frixione, P. Nason, and G. Ridolfi, JHEP **07**, 126 (2007); J.M. Campbell *et al.*, JHEP **1504**, 114 (2015); T. Je?o *et al.*, Eur. Phys. J. **C76**, 691 (2016);.
17. S. Frixione *et al.*, JHEP **06**, 092 (2006); S. Frixione *et al.*, JHEP **08**, 029 (2008); S. Alioli *et al.*, JHEP **09**, 111 (2009); E. Re, Eur. Phys. J. **C71**, 1547 (2011); R. Frederix, E. Re, and P. Torrielli, JHEP **12**, 130 (2012); R. Frederix *et al.*, JHEP **06**, 027 (2016).
18. S. Frixione and B.R. Webber, JHEP **02**, 029 (2002).

19. P. Nason, JHEP **04**, 040 (2004).
20. E. Todesco and J. Wenninger, Phys. Rev. Accel. Beams **20**, 081003 (2017).
21. V.M. Abazov *et al.* (DØ Collab.), Phys. Rev. **D94**, 092004 (2016).
22. T. Aaltonen *et al.* (CDF Collab.), Phys. Rev. **D88**, 091103 (2013).
23. T. Aaltonen *et al.* (CDF and DØ Collab.), Phys. Rev. **D89**, 072001 (2014).
24. T. Aaltonen *et al.* (CDF Collab.), Phys. Rev. **D89**, 091101 (2014).
25. V.M. Abazov *et al.* (DØ Collab.), Phys. Rev. **D90**, 092006 (2014).
26. G. Aad *et al.* (ATLAS Collab.), Eur. Phys. J. **C74**, 3109 (2014).
27. ATLAS Collab., ATLAS-CONF-2011-121.
28. G. Aad *et al.* (ATLAS Collab.), JHEP **1205**, 059 (2012).
29. ATLAS Collab., ATLAS-CONF-2011-140.
30. ATLAS Collab., ATLAS-CONF-2012-024.
31. ATLAS Collab., ATLAS-CONF-2012-031.
32. G. Aad *et al.* (ATLAS Collab.), Eur. Phys. J. **C73**, 2328 (2013).
33. G. Aad *et al.* (ATLAS Collab.), Phys. Lett. **B717**, 89 (2012).
34. S. Chatrchyan *et al.* (CMS Collab.), JHEP **11**, 067 (2012).
35. S. Chatrchyan *et al.* (CMS Collab.), Phys. Lett. **B720**, 83 (2013).
36. S. Chatrchyan *et al.* (CMS Collab.), JHEP **1305**, 065 (2013).
37. S. Chatrchyan *et al.* (CMS Collab.), Phys. Rev. **D85**, 112007 (2012).
38. S. Chatrchyan *et al.* (CMS Collab.), Eur. Phys. J. **C73**, 2386 (2013).
39. ATLAS & CMS Collabs., ATLAS-CONF-2012-134, CMS PAS TOP-12-003.
40. G. Aad *et al.* (ATLAS Collab.), Eur. Phys. J. **C76**, 642 (2016).
41. G. Aad *et al.* (ATLAS Collab.), Phys. Rev. **D91**, 112013 (2015).
42. ATLAS Collab., ATLAS-CONF-2017-054.
43. G. Aad *et al.* (ATLAS Collab.), Phys. Rev. **D95**, 072003 (2017).
44. V. Khachatryan *et al.* (CMS Collab.), Eur. Phys. J. **C77**, 15 (2017).
45. S. Chatrychyan *et al.* (CMS Collab.), JHEP **02**, 024 (2014).
46. V. Khachatryan *et al.* (CMS Collab.), JHEP **08**, 029 (2016).
47. V. Khachatryan *et al.* CMS Collab., Phys. Lett. **B739**, 23 (2014).
48. V. Khachatryan *et al.* CMS Collab., Eur. Phys. J. **C76**, 128 (2016).
49. ATLAS Collab., ATLAS-CONF-2014-053, CMS Collab., CMS-PAS-TOP-14-016.
50. R. Aaij *et al.*(LHCb Collab.), Phys. Rev. Lett. **115**, 112001 (2015).
51. ATLAS Collab., ATLAS-CONF-2015-033.
52. CMS Collab., CMS-PAS-TOP-15-005.
53. M. Aaboud *et al.*(ATLAS Collab.), Phys. Rev. **B761**, 136 (2016).
54. ATLAS Collab., ATLAS-CONF-2015-049.
55. V. Khachatryan *et al.*(CMS Collab.), Eur. Phys. J. **C77**, 172 (2017).
56. A. Sirunyan *et al.*(CMS Collab.), JHEP **1709**, 051 (2017).
57. CMS Collab., CMS-PAS-TOP-16-013.
58. CMS Collab., CMS-PAS-TOP-16-023.
59. A. Sirunyan *et al.* (CMS Collab.), `arXiv:1709.07411`, submitted to Phys. Rev. Lett..
60. ATLAS Collab., ATLAS-CONF-2011-108.

61. V.M. Abazov *et al.* (DØ Collab.) Phys. Rev. Lett. **107**, 121802, (2011); D. Acosta *et al.* (CDF Collab.) Phys. Rev. Lett. **95**, 102002, (2005).
62. V. Khachatryan *et al.* (CMS Collab.), Phys. Lett. **B736**, 33 (2014).
63. V.M. Abazov *et al.* (DØ Collab.), Phys. Rev. **D67**, 012004 (2003).
64. T. Affolder *et al.* (CDF Collab.), Phys. Rev. **D64**, 032002 (2001).
65. M. Czakon, D. Heymes, A. Mitov, Phys. Rev. Lett. **116**, 082003 (2016).
66. T. Aaltonen *et al.* (CDF Collab.), Phys. Rev. Lett. **110**, 121802 (2013).
67. G. Aad *et al.* (ATLAS Collab.), Eur. Phys. J. **C73**, 2261 (2013).
68. G. Aad *et al.* (ATLAS Collab.), Phys. Rev. **D90**, 072004 (2014).
69. G. Aad *et al.* (ATLAS Collab.), JHEP **06**, 100 (2015).
70. S. Chatrchyan *et al.* (CMS Collab.), Eur. Phys. J. **C73**, 2339 (2013).
71. M. Aaboud *et al.* (ATLAS Collab.), Phys. Rev. **D94**, 092003 (2016).
72. G. Aad *et al.* (ATLAS Collab.), Eur. Phys. J. **C76**, 538 (2016).
73. G. Aad *et al.* (ATLAS Collab.), Phys. Rev. **D93**, 032009 (2016).
74. V. Khachatryan *et al.* (CMS Collab.), Phys. Rev. **D94**, 052006 (2016).
75. V. Khachatryan *et al.* (CMS Collab.), Eur. Phys. J. **C77**, 459 (2017).
76. V. Khachatryan *et al.* (CMS Collab.), Phys. Rev. **D94**, 072002 (2016).
77. S. Chatrchyan *et al.* (CMS Collab.), Eur. Phys. J. **C75**, 542 (2015).
78. V. Khachatryan *et al.* (CMS Collab.), Eur. Phys. J. **C76**, 128 (2016).
79. M. Aaboud *et al.* (ATLAS Collab.), Eur. Phys. J. **C77**, 292 (2017).
80. CMS Collab., CMS-PAS-TOP-15-010 (2015).
81. ATLAS Collab., `arXiv:1708.00727 [hep-ex]`, submitted to JHEP.
82. ATLAS Collab., ATLAS-CONF-2016-100.
83. CMS Collab., CMS-TOP-16-007, submitted to JHEP.
84. V. Khachatryan *et al.* (CMS Collab.), Phys. Rev. **D95**, 092001 (2017).
85. G. Aad *et al.* (ATLAS Collab.), Eur. Phys. J. **C76**, 11 (2016).
86. G. Aad *et al.* (ATLAS Collab.), JHEP **01**, 020 (2015).
87. S. Chatrchyan *et al.* (CMS Collab.), Eur. Phys. J. **C74**, 3014 (2014).
88. S. Chatrchyan *et al.* (CMS Collab.), Phys. Lett. **B746**, 132 (2015).
89. G. Aad *et al.* (ATLAS Collab.), Phys. Rev. **D92**, 072005 (2015).
90. V.M. Abazov *et al.* (DØ Collab.), Phys. Rev. Lett. **103**, 092001 (2009); V.M. Abazov *et al.* (DØ Collab.), Phys. Rev. **D78**, 12005 (2008); V.M. Abazov *et al.* (DØ Collab.), Phys. Rev. Lett. **98**, 181802 (2007).
91. T. Aaltonen *et al.* (CDF Collab.), Phys. Rev. Lett. **103**, 092002 (2009); T. Aaltonen *et al.* (CDF Collab.), Phys. Rev. **D81**, 072003 (2010).
92. T. Aaltonen *et al.* (CDF Collab.), Phys. Rev. **D82**, 112005 (2010).
93. A. Heinson and T. Junk, Ann. Rev. Nucl. and Part. Sci. **61**, 171 (2011).
94. Tevatron Electroweak Working Group, `arXiv:0908.2171 [hep-ex]`.
95. CDF Collab., CDF conference note 11113 (2014), DØ Collab., DØ conference note 6448 (2014).
96. T. Aaltonen *et al.* (CDF and DØ Collab.), Phys. Rev. Lett. **115**, 152003 (2015).
97. T. Aaltonen *et al.* (CDF and DØ Collab.), Phys. Rev. Lett. **112**, 231803 (2014).
98. G. Aad *et al.*, ATLAS Collab., Phys. Rev. **D90**, 112006 (2014).
99. G. Aad *et al.*, ATLAS Collab., Phys. Lett. **B717**, 330 (2012).

100. S. Chatrychan *et al.*, CMS Collab., JHEP **12**, 035 (2012).
101. M. Aaboud *et al.*, ATLAS Collab., Eur. Phys. J. **C77**, 531 (2017).
102. S. Chatrychan *et al.* (CMS Collab.), JHEP **06**, 090 (2014).
103. CMS Collab., CMS-TOP-15-007.
104. M. Aaboud *et al.* (ATLAS Collab.), JHEP **04**, 086 (2017).
105. *et al.*(CMS Collab.), arXiv:1610.00678 [hep-ex], accepted by Phys. Lett. B.
106. C.D. White *et al.*, JHEP **11**, 74 (2009).
107. S. Frixione *et al.*, JHEP **07**, 29 (2008).
108. G. Aad *et al.* (ATLAS Collab.), Phys. Lett. **B716**, 142 (2012).
109. S. Chatrychan *et al.* (CMS Collab.), Phys. Rev. Lett. **110**, 022003 (2012).
110. G. Aad *et al.*(ATLAS Collab.), JHEP **01**, 064 (2016).
111. S. Chatrychan *et al.* (CMS Collab.), Phys. Rev. Lett. **112**, 231802 (2014).
112. ATLAS Collab., ATLAS-CONF-2014-052, CMS Collab., CMS-PAS-TOP-14-009.
113. M. Aaboud *et al.* (ATLAS Collab.), arXiv:1612.07231, submitted to JHEP.
114. CMS Collab., CMS-PAS-TOP-17-018.
115. ATLAS Collab., ATLAS-CONF-2011-118.
116. G. Aad *et al.*, ATLAS Collab., Phys. Lett. **B756**, 228 (2016).
117. V. Khachatryan *et al.*(CMS Collab.), JHEP **09**, 027 (2016).
118. CMS Collab., CMS-PAS-TOP-14-004.
119. CMS Collab., CMS-PAS-TOP-13-001.
120. CMS Collab., CMS-PAS-TOP-13-004.
121. ATLAS Collab., ATLAS-CONF-2016-012.
122. M. Czakon, P. Fiedler, and A. Mitov Phys. Rev. Lett. **115**, 052001 (2015).
123. W. Hollik & D. Pagani Phys. Rev. **D84**, 093003 (2011).
124. W. Bernreuther & Z.G. Si, Phys. Rev. **D86**, 034026 (2012).
125. S. Jung, H. Murayama, A. Pierce, J.D. Wells, Phys. Rev. **D81**, 015004 (2010).
126. V.M. Abazov *et al.* (DØ Collab.), Phys. Rev. Lett. **100**, 142002 (2008).
127. T. Aaltonen *et al.* (CDF Collab.), Phys. Rev. Lett. **101**, 202001 (2008).
128. CDF & DØ Collaborations, arXiv:1709.04894.
129. G. Aad *et al.* (ATLAS Collab.), JHEP **02**, 107 (2014).
130. G. Aad *et al.* (ATLAS Collab.), Eur. Phys. J. **C76**, 87 (2016).
131. G. Aad *et al.* (ATLAS Collab.), Phys. Rev. **D94**, 032006 (2016).
132. S. Chatrchyan *et al.* (CMS Collab.), Phys. Lett. **B717**, 129 (2012).
133. V. Khachatryan *et al.* (CMS Collab.), Phys. Rev. **D93**, 034014 (2016).
134. V. Khachatryan *et al.* (CMS Collab.), Phys. Lett. **B757**, 154 (2016).
135. G. Aad *et al.* (ATLAS Collab.), Phys. Lett. **B756**, 52 (2016).
136. G. Aad *et al.* (ATLAS Collab.), JHEP **05**, 061 (2015).
137. S. Chatrchyan *et al.* (CMS Collab.), JHEP **04**, 191 (2014).
138. CMS and ATLAS Collaborations, arXiv:1709.05327.
139. V.M. Abazov *et al.* (DØ Collab.), Phys. Rev. **D90**, 072001 (2014).
140. V.M. Abazov *et al.* (DØ Collab.), Phys. Rev. **D88**, 112002 (2013).
141. T. Aaltonen *et al.* (CDF Collab.), Phys. Rev. **D88**, 072003 (2013).
142. G. Aad *et al.* (ATLAS Collab.), Eur. Phys. J. **C72**, 2039 (2012).

143. F. Abe *et al.* (CDF Collab.), Phys. Rev. **D50**, 2966 (1994).
144. A. Abulencia *et al.* (CDF Collab.), Phys. Rev. **D73**, 032003 (2006).
145. G. Aad *et al.* (ATLAS Collab.), Eur. Phys. J. **C75**, 75 (2015).
146. V. Khachatryan *et al.* (CMS Collab.), Phys. Rev. **D93**, 072004 (2016).
147. V.M. Abazov *et al.* (DØ Collab.), Nature **429**, 638 (2004).
148. K. Kondo *et al.*, J. Phys. Soc. Jpn. **G62**, 1177 (1993).
149. R.H. Dalitz and G.R. Goldstein, Phys. Rev. **D45**, 1531 (1992); Phys. Lett. **B287**, 225 (1992); Proc. Royal Soc. London **A445**, 2803 (1999).
150. V.M. Abazov *et al.* (DØ Collab.), Phys. Rev. Lett. **113**, 032002 (2014).
151. L. Sonnenschein, Phys. Rev. **D73**, 054015 (2006).
152. CMS Collab. CMS-TOP-15-008 arXiv:1704.06142.
153. C.G. Lester & D.J. Summers, Phys. Lett. **B463**, 99 (1999).
154. CMS Collab., CMS-PAS-TOP-14-014.
155. CMS Collab., CMS PAS TOP-14-010.
156. B. Abbot *et al.* (DØ Collab.), Phys. Rev. **D60**, 052001 (1999); F. Abe *et al.* (CDF Collab.), Phys. Rev. Lett. **82**, 271 (1999).
157. T. Aaltonen *et al.* (CDF Collab.), Phys. Rev. **D92**, 032003 (2015).
158. G. Aad *et al.* (ATLAS Collab.), arXiv:1702.07546.
159. CMS Collab., CMS-PAS-TOP-17-007.
160. T. Aaltonen *et al.* (CDF Collab.), Phys. Rev. **D90**, 091101R, (2014).
161. A. M. Sirunyan *et al.* (CMS Collab.), Eur. Phys. J. **C77**, 354, (2017).
162. T. Aaltonen *et al.* (CDF Collab.), Phys. Lett. **B698**, 371 (2011).
163. CMS Collab., CMS PAS TOP-12-030.
164. V. Khachatryan *et al.* (CMS Collab.), Phys. Rev. **D93**, 092006 (2016).
165. V. Khachatryan *et al.* (CMS Collab.), JHEP **12**, 123 (2016).
166. CMS Collab., CMS-PAS-TOP-15-002.
167. CMS Collab., CMS-PAS-TOP-16-002.
168. T. Aaltonen *et al.* (CDF Collab.), Phys. Rev. **D80**, 051104, (2009).
169. V.M. Abazov *et al.* (DØ Collab.) Phys. Rev. Lett. **100**, 192004, (2008); S. Chatrchyan, (CMS Collab.), Phys. Lett. **B728**, 496, (2013);
V.M. Abazov *et al.* (DØ Collab.) Phys. Lett. **B703**, 422, (2011);
ATLAS Collab., ATLAS-CONF-2011-054;
U. Langenfeld, S. Moch, and P. Uwer, Phys. Rev. **D80**, 054009 (2009).
170. G. Aad *et al.* (ATLAS Collab.) JHEP **1510**, 121 (2015).
171. CMS Collab., CMS-PAS-TOP-13-006.
172. CDF Collab., CDF conference note 11080 (2014).
173. V.M. Abazov *et al.* (DØ Collab.), Phys. Rev. **D91**, 112003 (2015).
174. The Tevatron Electroweak Working Group, For the CDF and DØ Collab., arXiv:1608.01881.
175. ATLAS & CMS Collabs., ATLAS-CONF-2013-102, CMS PAS TOP-13-005.
176. M. Beneke *et al.*, arXiv:1605.03609.
177. A. H. Hoang *et al.*, JHEP **1709**, 099 (2017).
178. G. Aad *et al.* (ATLAS Collab.), Phys. Lett. **B716**, 1 (2012).
179. S. Chatrychyan *et al.* (CMS Collab.), Phys. Lett. **B716**, 30 (2012).

180. G. Degrassi, *et al.* JHEP **08**, 98, (2012).
181. S. Alekhin, A. Djouadi, and S. Moch., Phys. Lett. **B716**, 214, (2012).
182. T. Aaltonen *et al.* (CDF Collab.), Phys. Rev. **D87**, 052013 (2013).
183. V.M. Abazov *et al.* (DØ Collab.), Phys. Rev. **D84**, 052005 (2011).
184. G. Aad *et al.* (ATLAS Collab.), Phys. Lett. **B728**, 363 (2014).
185. S. Khatrychyan *et al.* (CMS Collab.), JHEP **06**, 109 (2012).
186. S. Khatrychyan *et al.* (CMS Collab.), Phys. Lett. **B04**, 028 (2017).
187. G. Mahlon and S. Parke, Phys. Rev. **D53**, 4886 (1996);
G. Mahlon and S. Parke, Phys. Lett. **B411**, 173 (1997).
188. G.R. Goldstein, in *Spin 96: Proceedings of the 12th International Symposium on High Energy Spin Physics,* Amsterdam, 1996, ed. C.W. Jager (World Scientific, Singapore, 1997), p. 328.
189. T. Stelzer and S. Willenbrock, Phys. Lett. **B374**, 169 (1996).
190. W. Bernreuther *et al.* Nucl. Phys. **B690**, 81 (2004).
191. A. Brandenburg, Z.G. Si, & P. Uwer, Phys. Lett. **B539**, 235 (2002).
192. V. Khachatryan *et al.* (CMS Collab.) Phys. Rev. **D93**, 052007 (2016).
193. CDF Collab., CDF conference note 10719 (2011).
194. CDF Collab., CDF conference note 10211 (2010).
195. V.M. Abazov *et al.* (DØ Collab.) Phys. Rev. Lett. **108**, 032004, (2012).
196. V.M. Abazov *et al.* (DØ Collab.), Phys. Rev. Lett. **107**, 032001 (2011).
197. V.M. Abazov *et al.* (DØ Collab.), Phys. Lett. **B702**, 16 (2011).
198. G. Mahlon & S.J. Parke, Phys. Rev. **D81**, 074024,2010.
199. G. Aad *et al.* (ATLAS Collab.) Phys. Rev. **D90**, 112016 (2014).
200. W. Bernreuther & Z.G. Si, Nucl. Phys. **B837**, 90 (2010).
201. G. Aad *et al.* (ATLAS Collab.) Phys. Rev. Lett. **114**, 142001 (2015).
202. G. Aad *et al.* (ATLAS Collab.) Phys. Rev. **D93**, 12002 (2016).
203. S. Chatrchyan *et al.* (CMS Collab.) Phys. Rev. Lett. **112**, 182001 (2014).
204. V. Khachatryan *et al.* (CMS Collab.) Phys. Lett. **B758**, 321 (2016).
205. G. Aad *et al.* (ATLAS Collab.) JHEP **03**, 113 (2017).
206. G. Aad *et al.* (ATLAS Collab.) Phys. Rev. Lett. **111**, 232002 (2013).
207. V.M. Abazov (DØ Collab.) Phys. Rev. **D95**, 011101R (2017).
208. V.M. Abazov *et al.* (DØ Collab.), Phys. Rev. **D92**, 052007 (2015).
209. A. Falk and M. Peskin, Phys. Rev. **D49**, 3320 (1994).
210. T. Aaltonen *et al.* (CDF Collab.), Phys. Rev. Lett. **111**, 202001 (2013).
211. CMS Collab., CMS-PAS-TOP-16-019.
212. M. Aaboud *et al.* (ATLAS Collab.), `arXiv:1709.04207`.
213. V.M. Abazov *et al.* (DØ Collab.) Phys. Rev. **D85**, 091104 (2012).
214. V. Khachatryan *et al.* (CMS Collab.) Phys. Lett. **B736**, 33 (2014).
215. G.L. Kane, G.A. Ladinsky, and C.P. Yuan, Phys. Rev. **D45**, 124 (1992).
216. A. Czarnecki, J.G. Korner, and J.H. Piclum, Phys. Rev. **D81**, 111503 (2010).
217. CDF and DØ Collab., Phys. Rev. **D85**, 071106 (2012).
218. CDF Collab., Phys. Rev. **D87**, 031103 (2013).
219. ATLAS Collab., JHEP **1206**, 088 (2012).
220. S. Chatrchyan *et al.* (CMS Collab.), JHEP **10**, 167 (2013).

221. ATLAS and CMS Collab., ATLAS-CONF-2013-033, CMS-PAS-TOP-11-025.
222. M. Aaboud *et al.* (ATLAS Collab.), Eur. Phys. J. **C77**, 264 (2017).
223. V. Khachatryan *et al.* (CMS Collab.), Phys. Lett. **B762**, 512 (2017).
224. CMS Collab., CMS-PAS-TOP-14-017.
225. S. Chatrchyan *et al.* (CMS Collab.), JHEP **01**, 053 (2015).
226. D. Choudhury, T.M.P. Tait, and C.E.M. Wagner, Phys. Rev. **D65**, 053002 (2002).
227. D. Chang, W.F. Chang, and E. Ma, Phys. Rev. **D59**, 091503 (1999), Phys. Rev. **D61**, 037301 (2000).
228. T. Aaltonen *et al.* (CDF Collab.), Phys. Rev. **D88**, 032003 (2013).
229. V.M. Abazov *et al.* (DØ Collab.), Phys. Rev. **D90**, 051101 (2014).
230. G. Aad *et al.* (ATLAS Collab.), JHEP **11**, 031 (2011).
231. CMS Collab., CMS-PAS-TOP-11-031.
232. T. Aaltonen *et al.* (CDF Collab.), Phys. Rev. **D84**, 031104 (2011).
233. G. Aad *et al.* (ATLAS Collab.), Phys. Rev. **D91**, 072007 (2015).
234. CMS Collab., arXiv:1706.08128.
235. ATLAS Collab., arXiv:1706.03046.
236. S. Chatrchyan *et al.* (CMS Collab.), Phys. Rev. Lett. **110**, 172002 (2013).
237. ATLAS Collab., ATLAS-CONF-2012-126.
238. G. Aad *et al.* (ATLAS Collab.), JHEP **1511**, 172 (2015).
239. V. Khachatryan *et al.* (CMS Collab.), JHEP **2016**, 96 (2016).
240. M. Aaboud *et al.* (ATLAS Collab.) Eur. Phys. J. **C77**, 40 (2017).
241. CMS Collab., CMS-PAS-TOP-17-005.
242. A. M. Sirunyan *et al.* (CMS Collab.) JHEP **07**, 003 (2017).
243. ATLAS Collab., ATLAS-CONF-2017-052.
244. CMS Collab., CMS-PAS-TOP-16-020.
245. S.P. Martin, `hep-ph/9709356` (1997).
246. C.T. Hill and E. Simmons, Phys. Reports **381**, 235 (2003).
247. C.T. Hill, Phys. Lett. **B266**, 419 (1991).
248. C.T. Hill, Phys. Lett. **B345**, 483 (1995).
249. V. Khachatryan, *et al.* (CMS Collab.), JHEP **11**, 154 (2014).
250. G. Aad *et al.* (ATLAS Collab.), JHEP **08**, 105 (2015).
251. CMS Coll. CMS PAS TOP-17-009.
252. ATLAS Coll. ATLAS CONF-2016-020.
253. C. Zhang and S. Willenbrock, Phys. Rev. **D83**, 034006 (2011).
254. J.A. Aguilar-Saavedra, Nucl. Phys. **B843**, 638 (2011).
255. V. Barger, T. Han, and D.G.E. Walker, Phys. Rev. Lett. **100**, 031801 (2008).
256. R. Frederix and F. Maltoni, JHEP **01**, 047 (2009).
257. T. Aaltonen *et al.* (CDF Collab.), Phys. Rev. Lett. **110**, 121802 (2013).
258. D. Acosta *et al.* (DØ Collab.), Phys. Rev. Lett. **94**, 211801 (2005).
259. T. Aaltonen *et al.* (CDF Collab.), Phys. Rev. **D84**, 072003 (2011).
260. A. Altheimer *et al.*, J. Phys. **G39**, 063001 (2012).
261. A. M. Sirunyan *et al.*(CMS Collab.), JHEP **1707**, 011 (2017).
262. G. Aad *et al.* (ATLAS Collab.), Phys. Rev. **D88**, 012004 (2013).

263. G. Aad *et al.* (ATLAS Collab.), JHEP **1508**, 148 (2015).
264. G. Aad *et al.* (ATLAS Collab.), JHEP **1301**, 116 (2013).
265. T. Plehn *et al.*, JHEP **1010**, 078 (2010).
266. A. M. Sirunyan *et al.*(CMS Collab.), arxiv:1708.08439.
267. A. M. Sirunyan *et al.*(CMS Collab.) arXiv:1708.01062.
268. A. M. Sirunyan *et al.*(CMS Collab.)JHEP **1708**, 073 (2017).
269. A. M. Sirunyan *et al.*(CMS Collab.) Phys. Lett. **B772**, 634 (2017).
270. V. Khachatryan *et al.*(CMS Collab.) Phys. Lett. **B771**, 80 (2017).
271. A. M. Sirunyan *et al.*(CMS Collab.) JHEP **1704**, 136 (2017).
272. A. M. Sirunyan *et al.*(CMS Collab.) JHEP **1705**, 029 (2017).
273. G. Aad *et al.* (ATLAS Collab.), Phys. Rev. **D86**, 091103 (2012).
274. G. Aad *et al.* (ATLAS Collab.), JHEP **11**, 104 (2014).
275. T. Plehn and T.M.P. Tait, J. Phys. **G36**, 075001 (2009).
276. CMS Collab., CMS-PAS-TOP-12-042 (2013).
277. V. Khachatryan *et al.* (CMS Collab.), JHEP **06**, 121 (2015).
278. A. M. Sirunyan *et al.*(CMS Collab.) arxiv:1706.02581.
279. G. Aad *et al.* (ATLAS Collab.), Phys. Rev. Lett. **108**, 041805 (2012).
280. J.A. Aguilar-Saavedra, Acta Phys. Polon. **B35**, 2695 (2004).
281. V. Khachatryan *et al.*, JHEP **02**, 028 (2017).
282. CMS Collab., CMS-PAS-TOP-14-003.
283. CMS Collab. CMS-PAS-TOP-17-003.
284. V. Khachatryan *et al.*, JHEP **02**, 079 (2017).
285. G. Aad *et al.* (ATLAS Collab.), arxiv:1509.00294.
286. G. Aad *et al.* (ATLAS Collab.), Phys. Lett. **B712**, 351 (2012).
287. A. Heister *et al.* (ALEPH Collab.), Phys. Lett. **B543**, 173 (2002); J. Abdallah *et al.* (DELPHI Collab.), Phys. Lett. **B590**, 21 (2004); P. Achard *et al.* (L3 Collab.), Phys. Lett. **B549**, 290 (2002); G. Abbiendi *et al.* (OPAL Collab.), Phys. Lett. **B521**, 181 (2001).
288. F.D. Aaron *et al.* (H1 Collab.), Phys. Lett. **B678**, 450 (2009).
289. H. Abramowics *et al.* (ZEUS Collab.), Phys. Lett. **B708**, 27 (2012).
290. M. Beneke *et al.*, hep-ph/0003033, in *Proceedings of 1999 CERN Workshop on Standard Model Physics (and more) at the LHC*, G. Altarelli and M.L. Mangano eds.
291. V.F. Obraztsov, S.R. Slabospitsky, and O.P. Yushchenko, Phys. Lett. **B426**, 393 (1998).
292. T. Carli, D. Dannheim, and L. Bellagamba, Mod. Phys. Lett. **A19**, 1881 (2004).
293. V.M. Abazov *et al.* (DØ Collab.), Phys. Rev. Lett. **102**, 092002 (2009).
294. V.M. Abazov *et al.* (DØ Collab.), DØ conference note 5838 (2009).
295. V.M. Abazov *et al.* (DØ Collab.), Phys. Lett. **B708**, 21 (2012).
296. ATLAS Collab., ATLAS-CONF-2013-032.
297. T. Aaltonen *et al.* (CDF Collab.), Phys. Rev. Lett. **101**, 192002 (2009).
298. V.M. Abazov *et al.* (DØ Collab.), Phys. Lett. **B701**, 313 (2011).
299. V.M. Abazov *et al.* (DØ Collab.), Phys. Lett. **B693**, 81 (2010).
300. S. Chatrchyan*et al.*(CMS Collab.), Phys. Rev. Lett. **112**, 171802 (2014).

301. A. Sirunyan *et al.*, JHEP **07**, 003 (2017).
302. G. Aad *et al.* (ATLAS Collab.), Eur. Phys. J. **C76**, 12 (2016).
303. G. Aad *et al.* (ATLAS Collab.), JHEP **1209**, 139 (2012).
304. G. Aad *et al.* (ATLAS Collab.), JHEP **1512**, 061 (2015).